2018

Electroplating of Copper on Tungsten Powder

Richard Berdos

ELECTROPLATING OF COPPER ON TUNGSTEN POWDER

A Thesis Presented

By

RICHARD F. BERDOS

Submitted to the Graduate School of the
University of Massachusetts Amherst in partial fulfillment
of the requirements for the degree of

MASTER OF SCIENCE IN MECHANICAL ENGINEERING

September 2018

Mechanical Engineering

ELECTROPLATING OF COPPER ON TUNGSTEN POWDER

A Thesis Presented

by

RICHARD F. BERDOS

Approved by:

_____

Robert W. Hyers, Chair

_____

Stephen S. Nonnenmann, Member

_____

David P. Schmidt, Member

_____

Sundar Krishnamurty, Department Head
Mechanical & Industrial Engineering

ACKNOWLEDGEMENTS

I would first like to acknowledge my thesis advisor Professor Robert Hyers. Thank you, Bob. Without your guidance and support, I would not have been able to gain the necessary knowledge to complete and write this thesis. I have learned so much from you both in the classroom and during this thesis, and I am very appreciative for the dedication that you had towards me in achieving this goal.

I would also like to thank the members of my thesis committee: Professor Stephen S. Nonnenmann and Professor David P. Schmidt for their assistance and guidance throughout the process. Thank you, Michael Jercinovic for your kindness and assistance in showing me the ropes of SEM analysis. Thank you to Al Rakoukas for all the laboratory assistance.

I'd like to thank my mother and father, Lori and Peter Berdos, and my brother, Peter Berdos, for your love and support throughout my college career. Thank you, Anna Plewa, Michael Frey, Gwendolyn Bracker, and the rest of my amazing family and friends. This accomplishment would not have been possible without you. Finally, thank you to the Army Research Lab, this project would not have been possible without your support.

ABSTRACT

COPPER PLATING TUNGSTEN POWDER BY ELECTRODEPOSITION

SEPTEMBER 2018

RICHARD F. BERDOS

B.S., UNIVERSITY OF MASSACHUSETTS AMHERST

M.S.M.E. UNIVERSITY OF MASSACHUSETTS AMHERST

Directed by: Professor Robert W. Hyers

Strengthening, resistant and shielding properties, to name a few, can be achieved by implementing a surface material coating onto an engineering component. Various elements of these compounded parts can augment the functionality of the part, such as, increased life time and more interactive surfaces. Tungsten has proven to be a challenge to plate with other metals, but if done correctly, the results can allow for the cold spray of tungsten. Cold spraying tungsten particles alone provides a challenge because the powder is too hard and instead of adhering, it erodes the surface it is attempting to plate. Coating tungsten in a softer metal, like copper, will allow for the particles to adhere to the surface and create a strengthened and radiation shielded component. It also yields a better surface to electroplate onto in the future, as tungsten itself is hard to plate onto, so the copper layer provides the ability to easily plate other metals.

The purpose of this thesis project is to encapsulate tungsten powder within copper, then scale up the process to produce bulk amounts of the material in a batch process. The particles will be encased using an electroplating method, that has been

turned into a semi-autonomous process for the ease of producing bulk powder. While electroless deposition has previously shown positive results for attaining a uniform coating, making it a semi-batch process for bulk material would have an extreme cost in comparison to electrolytic deposition. The tungsten particles have been successfully enclosed in copper by electrolytic deposition in this set of experimentation using an HF electro-etch pretreatment and ultrasonic agitation during electroplating. Further experimentation will include improved methods of stirring and transferring powder, as the transfer takes too long between the etch and the onset of plating and the stirring method is bulky and reduces the area that can be efficiently plated on.

TABLE OF CONTENTS

APPENDICES

LIST OF TABLES

LIST OF FIGURES

CHAPTER 1

INTRODUCTION

1.1   Purpose

Desirable material properties can be gained as the result of coating a component with a surface material. In some cases, these surface coatings can provide different abilities, such as added strength, solderability, and wear resistance. The purpose of this thesis is to explore various methods for plating tungsten (W from Buffalo Tungsten), with copper, for a proprietary application. The grains of powder are being encased using an electroplating method, invented by Pay Yih (patent # 5,911,865) in 1997 [1]. A copper coating on the tungsten powder will give it a better chance to bond to a metal surface in a cold spray process. Copper is a softer metal that makes the deformation of particles more favorable, which is a key to the success for bonding in the cold spray coating process. Metals have been applied to the surface of materials for various reasons, like adjusting the friction coefficient of the surface and to provide a new layer of wear resistant material [2].

1.2   Thesis Outline

The background information regarding this thesis is found in the form of a literature review in Chapter 2; the chapter covers: cold spray, tungsten, mechanics, electroplating of copper, and calculations used to initialize and evaluate the experiments. Chapter 3 describes the results from completed experiments, including all the macroscopic and microscopic substrate tests with all the pretreatments. It includes details

regarding the experimental setup and an overview of result analysis. Chapter 4 provides a summary of the results and the experiments conducted throughout the study. Chapter 5 describes the conclusions that were able to be drawn from the experiments, while Chapter 6 describes further testing that should be conducted to attempt to find a more efficient solution.

CHAPTER 2

BACKGROUND

2.1   Introduction

Metal plating has been used in many different applications over many years, like wear resistance, corrosion resistance, and enhanced engineering properties. Tungsten coating has also begun to emerge in the fire-proofing and anti-radiation industries, as it has a higher density than other popular anti-radiations materials, such as lead. However, its cost is much higher, leading to the use of tungsten only when the space for the radiation protection is less favorable for lead [3]. As for fire-proofing, tungsten has the highest melting point among all metals, not just the transition metals, and it can retain its strength at those high temperatures. Overall, tungsten's hardness and high density give it many functions, for general and military purposes, as a coating layer on a component.

Cold spray is a solid-state deposition process in which metal powder is propelled at high velocities and temperature well below the melting point of the material, causing particle deformation on impact that results in a strong metallurgical bond. The significant plastic deformation experienced by the particles forms an adiabatic shear instability upon contact, breaking down surface oxides. Due to this break, shear is developed at the contact interface and material is expelled from the contact. This shear between particles and at the spray contact interface causes the solid-state metallurgical bonding [4].

There are many modern metal spray techniques used throughout industry, Figure 1 demonstrates the operational threshold for each of the techniques. The cold

3

spray process operates at the lowest temperature of all the conventional spray techniques and the highest velocity. The high temperatures of plasma, detonation and High Velocity Oxygen Fuel (HVOF) create melted particles that shrink upon cooling. This leaves high tensile residual stresses. Due to the low temperatures of cold spray, the particles are not melted, resulting in a much smaller, and compressive, residual stress, in comparison to the other methods. The crystalline structure also remains mainly unchanged during deposition in cold spray, unlike the particles of the higher temperature depositions, which tend to change their crystalline structure upon resolidification [5].
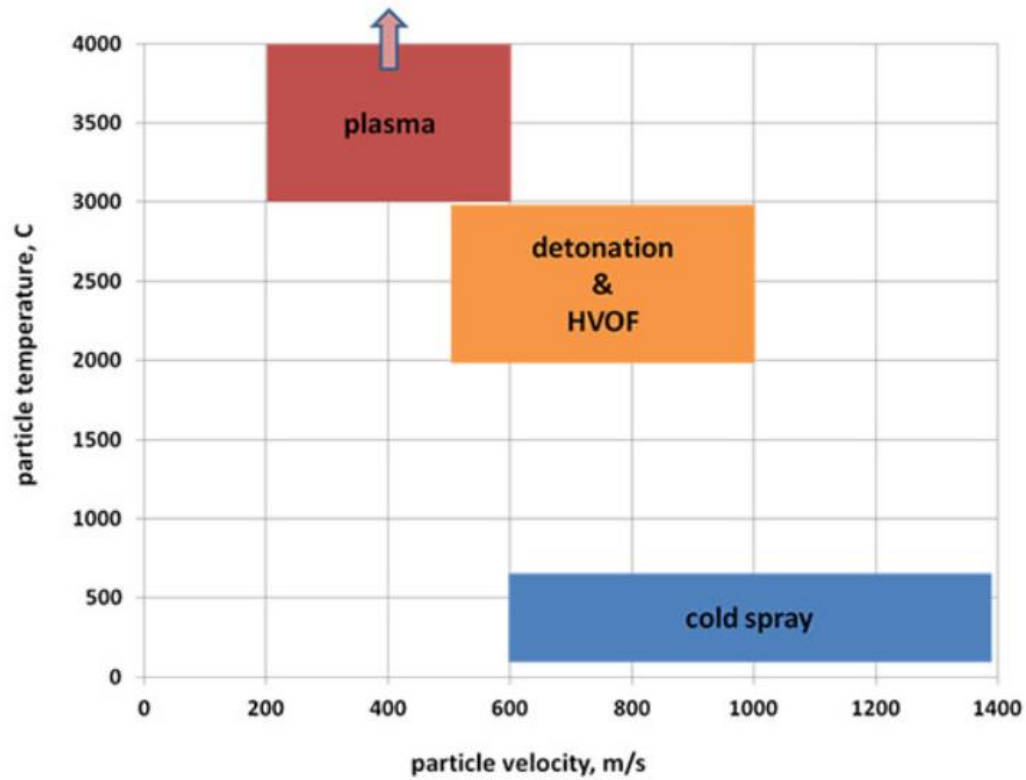
Figure 1: A view at the operating ranges for metal deposition coatings. Plasma, detonation and HVOF all operate at higher temperatures than cold spray, but detonation and HVOF have some velocity overlap with cold spray, whereas plasma is strictly low velocity application [5]

These various coating techniques have different effects on the appearance of the coating. The higher temperature coatings exhibit a much higher porosity in comparison to cold spray, which has <1% porosity. This difference is shown in Figure 2, a high temperature flame sprayed Sn coating, and Figures 3 and 4, which are cold spray coating examples.

5
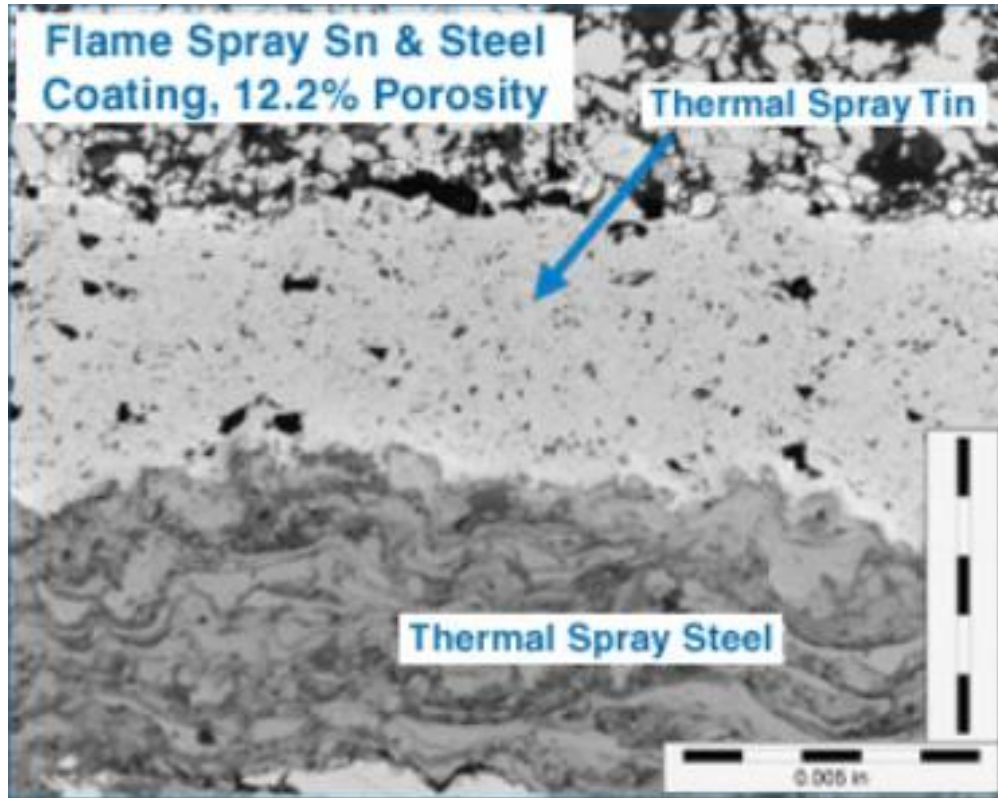
Figure 2: Flame spray deposition of Sn and Steel, with a coating porosity of 12.2%. This image was created using backscattered electron (BSE) imaging [5]
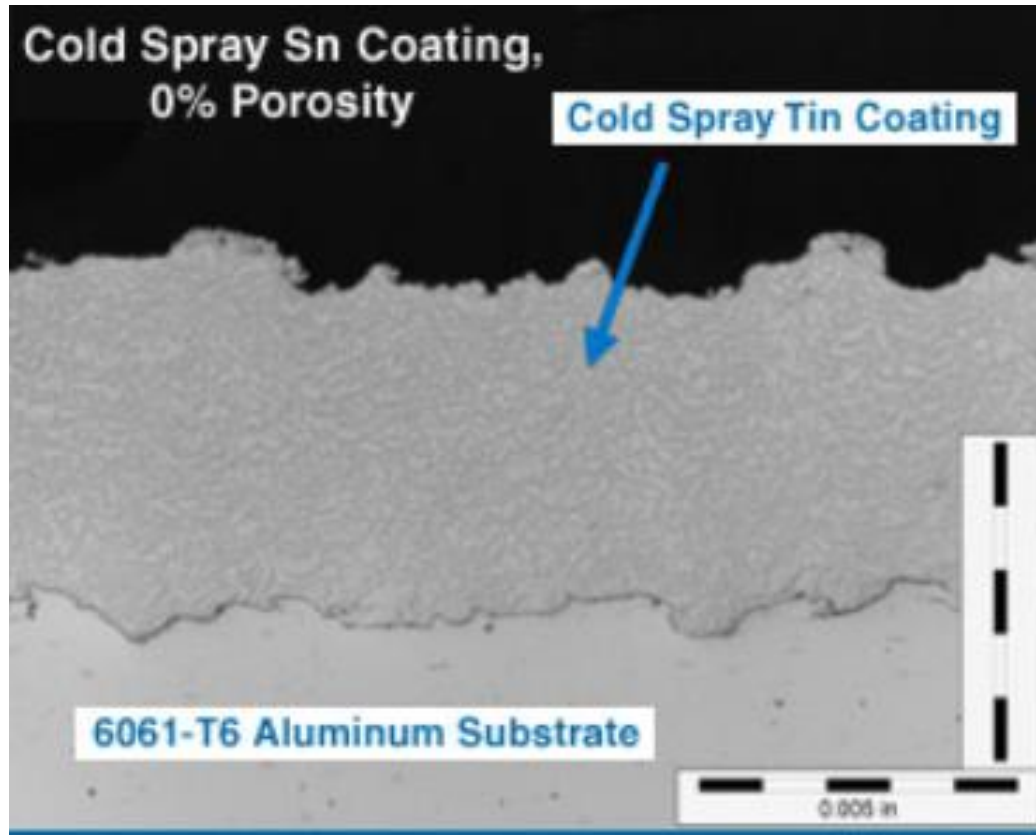
Figure 3: Aluminum substrate cold spray coated with Sn displaying a 0% porosity, viewed in a BSE image [5]
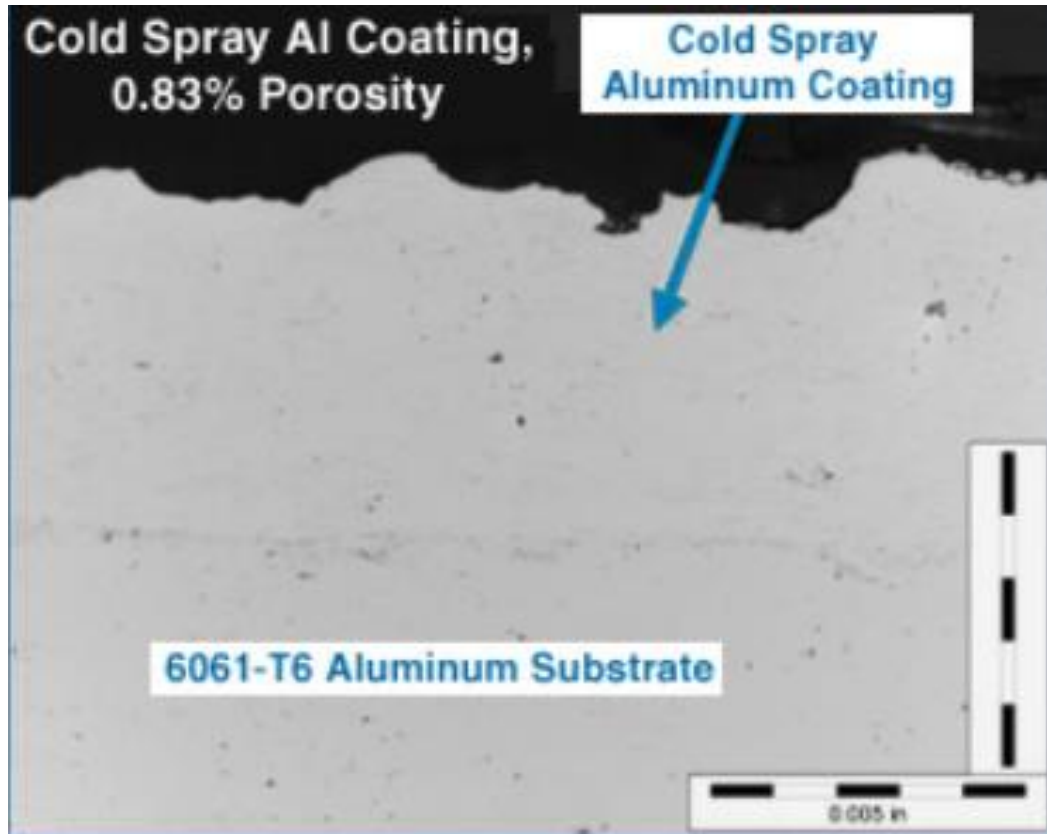
Figure 4: BSE image of aluminum substrate coated via cold spray with aluminum with a porosity of 0.83% [5]

2.2   Applications and Requirements

2.2.1   Tungsten (W)

W is a unique transition metal that is unparalleled by all materials in many categories, including the highest melting temperature and tensile strength. The powder used throughout these experiments was made by Buffalo Tungsten Inc. The particles had diameters in the range of 5-10 μm with an apparent density of 3.0-5.5 g/cc. W itself has many useful applications, including light bulb filaments, electrical contacts, heating elements, plastic densification, aiding in the production of tungsten carbide, and additive strengthening of steel. Among metals, tungsten has the highest melting point, the lowest coefficient of thermal expansion, and the lowest vapor pressure. It also has unusually high strength at extreme temperatures. These properties make it a desirable material to coat with, as its strength and durability at high temperatures make it unique for many military applications, as many bullets, missiles, and rocket parts are coated with forms of tungsten. Not only does it have these extraordinary properties, but they are coupled with other compelling characteristics, such as high resistance to corrosion, high modulus of elasticity, and high resistance to thermal creep [6].

The W particles, from Buffalo Tungsten, were blocky in shape, with a scatter of fused clusters. The surfaces are not particularly smooth, and the particles appear to have agglomerates on them. A closer look at the particles can be observed below in Figure 5.

9
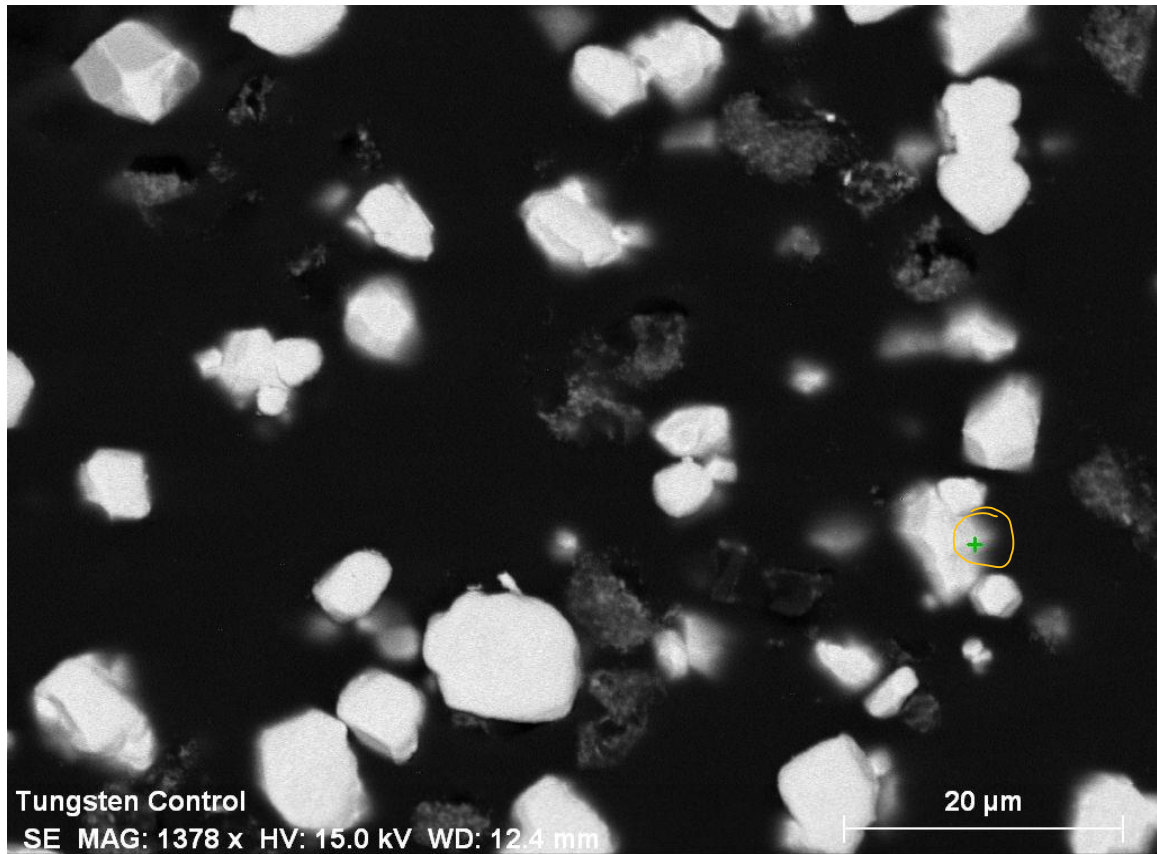
Figure 5: Image of W powder particle from a backscattered electron view. The powder particle was mounted in an epoxy puck, ground and polished, so that cross-sections of the particulate could be seen. The cloudy edges of the particles give it the appearance of being coated, so the particle was analyzed with EDS imaging to realize the makeup. The particular portion that was analyzed in this case is the plus sign in the yellow circle.

2.2.2 W composition

In an initial, control test, W particles were mounted into an epoxy resin and then ground and polished. Below, in Figure 5, W particles can be seen and the cloudy outline around the particle that can be easily mistaken for a coating in a backscatter image, is denoted with a plus sign. This spot marked by the sign was analyzed with energy dispersive x-ray spectroscopy (EDS), to reveal the elemental composition of the spot.

The resultant plot of the elemental composition is shown in Figure 6. The cloudy regions were shown to have only W and little to no traces of copper.
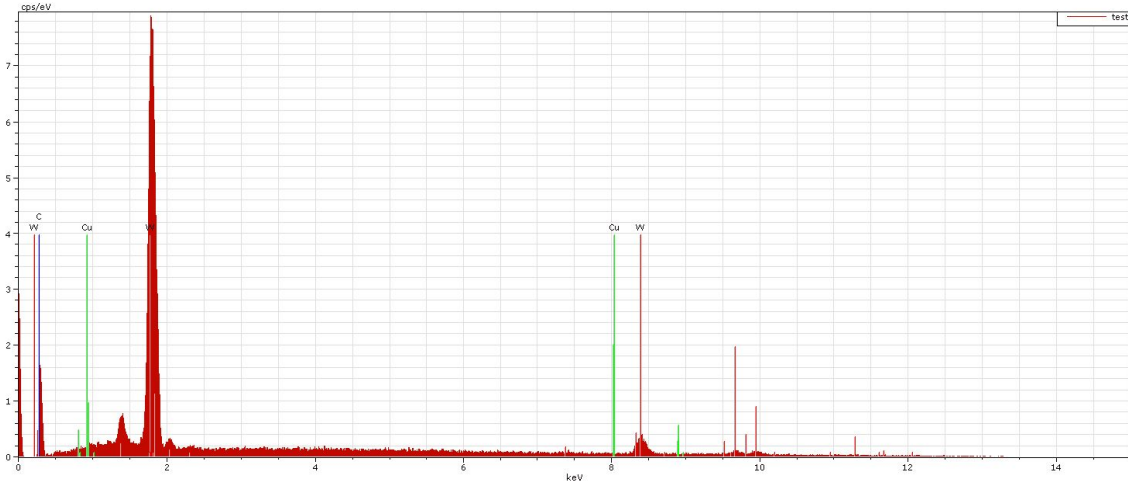
Figure 6: EDS spectra graph of W region that appeared to be coated in Figure 5. This figure shows that most of the W x-ray energy matches with the Mα x-rays and a smaller, insignificant amount with the Lα and Lβ x-rays, as the leftmost peak is the carbon from mounting, labeled with a C.

The figure above displays a high concentration of W on the left side of the figure, Mα x-rays and a smaller amount of W after at a smaller peak on the right, the Lα and Lβ x-rays. The even height, vertical lines throughout the image, denote the areas in which energies are expected for the specific elements. The lines are labeled with the element that correspond to that energy peak. These results are consistent with the concentration of W given by Buffalo Tungsten Inc. of 99.9% W in powder [7], as shown in Table 1 below.

Table 1: EDS results for the W powder particles compared to manufacturer safety data sheet (SDS)

Element	Series	Wt % (Fig 7)	Wt % (W particle center)	Wt % SDS
Tungsten	L-series	99.9%	99.9%	99.9%

2.2.3   W limiting factors for Cold Spray deposition

Cold spray has a large range of high velocities at which it can operate. At the high velocities of cold spray, the W particles can be moving too fast causing them to erode the surface of the substrate, instead of adhering to the surface. W is a harder particle that requires a higher velocity for cold spray, causing erosion to the substrate before bonding takes place. The coating of a hard material, in this case W, in a softer metal, that is more favorable for cold spray, minimizes erosion and increases the probability of adhesion. To achieve bonding between the W powder and another metal, the powder must be coated in copper. The copper allows the particle to undergo deformation at higher speeds, causing the composite powder to bond with the substrate, rather than erode it.

2.3   Method of coating particles

W powder particles need to be coated in copper to allow the deformation needed for successful bonding to another metal during a cold spray process. The approach that was investigated to turn the coating into a large scale, semi-batch process, was electroplating. Electroplating has many benefits over alternative methods, including, high coating efficiency and coating quality, an ability for a vast array of coating thickness, and a low cost in comparison with other plating methods.

In traditional electroplating, the cathode is a flat substrate. For electroplating powders, the approximately spherical particles must contact the cathode and only touch the cathode for a short duration of time to prevent bonding between the particles and the cathode by electroplating. The conventional electroplating process restricts deposition between particles under the surface layer through to the cathode. As the deposition was limited by the size of the particles, a more creative approach was needed to plate

12

powders, thus, a new method for achieving the result of electroplating powders was discovered by Dr. Pay Yih [1]. His device was designed with the intention of encasing metal powders and the technique became adopted by the Federal Technologies Group, a metal powder producer. Similar apparatuses and techniques also emerged, focused on different particle pretreatment methods and stirring modifications [8].

These deposited coatings can be achieved in other ways other than electroplating, such as electroless plating, and chemical and physical vapor deposition (CVD and PVD, respectively) processes. Electroless plating specifically can be very effective for achieving a uniform coating on the powder, however, in practice, the method results in too high of a cost to be competitive in a large-scale coating process. As for CVD and PVD, there is a limited set of coating materials, paired with even higher costs and a lower deposition rate.

2.3.1 Electroplating

Electroplating copper requires a direct current flow between two electrodes that are submerged in an aqueous solution of a copper salt. The cathode acts to reduce the Cu^{2+}, copper ions, that are present in the solution. The copper ions gain electrons and arrive at their neutral metal state to become deposited on the substrate. Simultaneously, the Cu at the anode is being oxidized by the current, transforming Cu to Cu^{2+} ions, and replenishing its concentration in the electrolyte solution. Electrons released from the anode take a path through the power supply to the cathode, where they interact with the copper ions at the cathode surface.

Throwing power provides a measure of a solutions ability to plate complex structures with inherent surface complexities. The throwing power of a solution is

13

determined by the ionic conductivity of the solution, current efficiency, and applied current density. High throwing power is associated with nearly equal plating thickness throughout the surface, regardless of the complexity. To increase the throwing power of the copper electrolyte solution, there are a variety of measures that can be taken. They include, increasing the electrical conductivity of the solution, raising the pH, lowering the current density, increasing the temperature, and increasing the distance between the electrodes that are submerged in the solution [9]. In parallel with throwing power is the ability of the solution to initiate plating on the cathode, known as covering power. This can occasionally be increased by pretreating the substrate, in this case, the W powder [9]. Throwing power and covering power are directly related, so ideally, the solution being used for depositing Cu on W would have high throwing and covering powers.

The aforementioned design for electroplating described in the patent [1], was designed for electroplating powders. A model of the device is shown below in Figure 7, this acted as a baseline for the experimental design used in this thesis.
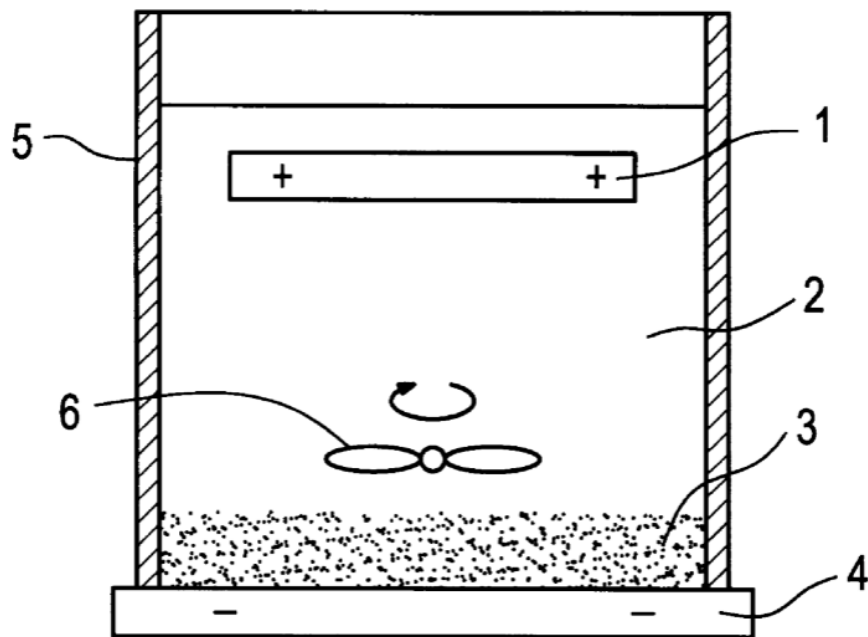
Figure 7: Dr. Pay Yih's electroplating device. Powder (3) is confined to a container (5), in this case a beaker, that contains an electrolyte solution (2) to connect the anode (1) and cathode (4) by direct current. When the particles settle on the cathode, a metal stirrer (6) disperses the particles to allow for an even plating of the powder [1].

This device presented many possible methods for plating the W particles. The first method was to apply the direct current between the anode (1) and cathode (4) while the magnetic stirrer (6) is mixing the powder (3) and solution (2) to plate the powder in copper. This method is seen as a standard electroplating method [2]. This would theoretically plate the particles as they settled back to the cathode, providing a uniform coating via electroplating, as the powder and solution would be theoretically uniform. There is a major drawback to this method though, that being that copper from the anode could be deposited on the copper cathode rather than on the particles in solution. Where this seems more trivial because the anode and cathode are the same composition, it would

15

cause a greater waste or "loss" of copper than the other methods, as the powder can only be plated when it is in electrical contact with the cathode.

The second method eliminates most of the copper waste seen in the first method. This method is also seen as a standard electroplating method [2,8]. In this method, the powder is stirred with the solution while no current is being applied between the electrodes. The particles are then allowed time to settle onto the cathode, providing a barrier between the electrodes. Once the powder is mostly settled, the current is applied, and the W particles will be encased in copper, as they form an electrical connection to the cathode. Ions get trapped between the powder as it settles and assist in making contact to the cathode, but when they do so, they are depleting the electrolyte solution. Bridging of the powder occurs at the top of the settled particle pile. This is when a single cycle of coating layer fuses two or more particles together. This can easily be prevented by coating with cyclic interrupts of the current and stirring of the particles, only exposing the top layer to the current and coating for short periods of time. The mixing component will allow new particles to resettle on the top and coat the new layer. This method is preferred over the first, not only for the better "loss" and cost properties, but also for the coating efficiency.

A third approach to electroplating using the apparatus is a hybrid between the first and second and theoretically would maximize plating efficiency. This method was presented to accompany the device in the patent [1,8]. In this method, the direct current is applied after the particles have been stirred and settled only enough that the cathode is completely covered. Plating can then occur on many layers in one cycle, as the initial layer will receive a coating when the current is first applied, and the others will slowly

16

receive a coating as they settle and encounter the powder pile. The loosely settled powder will have the trapped ions, much like in method two, however, these ions will be able to exist in greater quantities, closer to the cathode because of the falling particles continuing to trap them once plating has begun. This method will also allow for the electrolyte solution to remain present in the interparticle spaces unlike before. This allows the experiment to have an ideal thickness of sedimented W, that will allow for a maximal deposition on the powder, instead of the cathode. The ideal thickness of sedimentation is dependent on throwing power and covering power of the copper salt solution, the distance from the pinnacle layer of powder to the base of the submerged anode, usually greater than 5mm, density, morphology, and conductivity of the particulates.

The electroplating process can be strongly influenced by the electrolyte solution that it takes place in. Electrolyte solutions can be swayed to be higher throwing power solutions or lower based on concentrations and amounts of specific components in solution. The electrolyte solutions can be affected by pH changes, corresponding to the bath composition change, and temperature fluctuations. The average operating range for copper acid electroplating is between 18ºC and 60ºC and an acidic pH between 2 – 5 [2]. As the pH becomes too neutral, the throwing power decreases, and the surface of the deposit becomes rougher, which will decrease the plating efficiency of the solution [10].

Later experiments had the addition of an ultrasonic bath to increase the amount of agitation the particles experienced, and in turn, increase the plating efficiency [2]. When the ultrasonic bath was added, there was no longer a magnetic stirring option, so a new method of stirring was adapted. It involved the use of a corded power drill and a polypropylene paddle stirrer. The anode was a copper end fitting, instead of a bar, with a

17

hole drilled in it, so that the stirrer could be placed through it and reach the cathode to

mix the particles into the solution.

2.3.1.1 Equipment and personal safety equipment

Equipment:

- Fischer Scientific ISOTEMP hotplate with magnetic stirring
- Fischer Scientific Education scale and plastic weigh boats
- DC Power Supply
- 3/8" ID POLYSPRING® PVC Food and Beverage Vacuum hose KTM081027
- 1 x 400 mL glass beaker
- Branson 1500 Ultrasonic bath
- Black and Decker corded drill
- Chemical resistant T-shaped polypropylene paddle stirrer

Safety equipment:

- Long sleeve lab coat and safety goggles
- Powderless plastic gloves
- N95 particulate respirator
- For HF use see Appendix B for additional equipment

2.3.1.2 Experimental solution concentration

Each experiment began with mixing the electrolyte solution. Even though the

solution went through a vacuum filter at the end of the experiment, some residual

particles prevented the recycling of the electrolyte solution.

The solution itself was composed of two different ingredients, copper sulfate

($CuSO_4$) and hydrochloric acid (HCl) or sulfuric acid (H_2SO_4) [2]. The ingredients were

either measured on a Fischer Scientific Education Scale in plastic weigh boats, in the case

of the copper sulfate, or in a glass graduated cylinder, in the case of the HCl or H_2SO_4.

To maintain a constant solution composition through the experiments, large batch

18

solutions were made to use in smaller quantities over many experiments. The exact specifications of the solution used in testing were:

- 0.5M H_2SO_4 (28 mL) or 0.5M HCl (0.905 mL)

- 0.1M $CuSO_4$ (5.02 grams)

- pH 2-5

The pH was set closer to 2, as the lower pH solution had a higher throwing power and a better chance at achieving a successful result. To create the solution for a single test, the contents in Table 2, were mixed independently first in their own beakers using a glass stirring rod, then they were combined to create the test solution and were mixed on a Fisher Scientific ISOTEMP hotplate with a magnetic stir bar. This device was only used for its magnetic stirring and not for heating the solution. The solution mixed for an additional 10-15 minutes, until no copper sulfate particles remained.

Table 2: This table shows the solution composition for a 228mL electrolyte solution for electroplating copper that was used for initial testing.

Ingredients	Mass (g or ml)
Copper Sulfate	5.02 g
Hydrochloric Acid	0.905 mL
Sulfuric Acid	28 mL

In electroplating, the electrolyte solution is crucial to the results, as it must be carefully chosen to ensure that it does not react with the anode, cathode, or the powder that is to be plated or provide undesired elements in the results.

2.3.1.3 Experimental procedure

Following the standard electroplating procedure outline in Section 2.3.1, hundreds of cycles were used to encapsulate all the particles in copper, each cycle containing three steps. The three steps are comprised of stirring, sedimentation, and electroplating.

In the first step, the W particles were either agitated using the magnetic stirring bar, spinning at a rate of 1100 rpm or by the combination of the drill and paddle stirring when an ultrasonic bath was used for additional agitation. This step was intended to break up the particles and sever any copper bridges that may have formed between them in the last plating cycle. It created a uniform distribution of metal powder held in the electrolyte solution, while also randomizing the particles surface position for the best plating. As discussed above, it also diminishes the concentration gradient of copper ions suspended in solution that materialize due to the high current through the solution during the electroplating process.

In the second step, the stirring mechanism ceased and allowed for the uniform mix of W powder to relax and fall back toward the cathode. The theoretical calculation for sedimentation time is presented in Section 2.4.4, however, as described in that section, this procedure gave the particles more time, 100 seconds, to settle on the cathode before electroplating began. As the particles fell to rest loosely on the cathode, the electrolyte solution had an opportunity to move through spatial channels created by the

20

loose-fitting particles, so that it could interact with particles below the surface layer and closer to the cathode, allowing for copper deposition on more surfaces at once.

The final step was electroplating, where the HY 3003-3 DC power supply was connected in parallel and turned on to supply a direct current through the electrolyte solution and induce Cu deposition on the W particles. This step varied depending on how the test was run, as seen above in Section 2.3.1, as the particles did not have to be completely settled, or even settled at all for this step to commence. However, in the testing for this thesis experiment, the powder could fully settle on the cathode before inducing the current through the solution. Once the current was applied, the electroplating of Cu began by reducing the Cu and allowing the ions to deposit on the W powder. The cycle lasted for 60 seconds, upon which the power supply was shut off and the stirring step began the cycle again.

2.4   Calculations

The electroplating experiment carried out to deposit copper onto the W powder was evaluated theoretically with a series of equations. Rigali [11] summarizes many of the calculations relevant to planning and executing the plating process. These calculations were employed for the present system: Cu on W powder. These equations can guide the experimental setup and help to confirm experimental performance through means of calculations. The electroplating method was evaluated using these calculations to determine the proper experimental setup for achieving a desired thickness of copper that would encapsulate the W powder.

21

2.4.1 Calculate total deposition area

The total deposition area is a function of the total mass of the powder being encased in copper, the average particle diameter, assuming the particulates were spherical, and the density of the particles. The assumed diameter was used to derive the surface area for a single particle and then that result was multiplied by the total number of particles per unit mass. Equation 2-1,

$$A_s = 4\pi(\frac{D_p}{2})^2 * (\frac{m_t}{\rho_p * \frac{4\pi}{3}(\frac{D_p}{2})^3}) = \frac{6 * m_t}{\rho_p * D_p}, \tag{2-1}$$

presents a consolidated estimate of the initial surface area that copper was being deposited on, where A_s is surface area, m_t is total mass of encased powder, ρ_p is density of powder, and D_p is average particle diameter. For example, for a bulk process it is desired to produce at least one pound of powder. With a known total mass of approximately 454 g, a known density of W of 19.3 g/cm^3, and an average particle diameter of 20 μm, the surface area was calculated to be 7.04x10^4 cm^2. From here, the total amount of copper to be deposited on the surface area of tungsten is equivalent to the surface area multiplied by the desired thickness of the coating, under the assumption that the plating is uniform and contains 100% copper. This estimate also assumes that the plating is thin compared to the particle diameter. Sometimes thick coatings are also desired, the thickness of a thick coating is calculated below in Equation 2-2.

2.4.2 Calculate target plating thickness and volume

During the process of depositing the copper onto the W powder, the goal was to encase the W particles in 25 wt.% Cu. The electroplating of Cu onto W was expected to have a uniform thickness. To achieve 25 wt.% Cu, a third of the mass of W must be

22

deposited evenly onto the W particles. Once the added mass was determined, the particle

diameter after coating could be determined. Equation 2-2,

$$\delta = \frac{\left[\left(V_p + \frac{m_{Cu}}{\rho_{Cu}}\right)\frac{6}{\pi}\right]^{\frac{1}{3}} - D_0}{2},$$ (2-2)

where δ is deposited coat thickness, V_p is original particulate volume, m_{Cu} is mass of

25 wt.% copper, ρ_{Cu} is density of copper, and D_0 is original particle diameter. The mass

divided by density of copper term represents the volume of the added copper, making the

term in parenthesis the total volume of the encased particulate. Implementing

Equation 2-2 for an original particle diameter of 15 μm, the resulting thickness was

1.481 μm. This calculation was carried out with a V_p=1.76x10^{-09} cm^3, under the assumption

that the particles were perfect spheres, and an m_{Cu}=1.14x10^{-08} grams, derived from the

mass of the particle after coating minus the mass of the particle before coating. The volume

of Cu added to the powder is simply the mass over the density component from the above

equation, and the new particle volume is that term plus the V_p, in this case, that total was

3.03x10^{-09} cm^3.

2.4.3 Electroplating

In electroplating, it is important to know the current or time associated with

certain plating thicknesses and how to achieve that thickness with one of the two

variables constant. To calculate this, a few initial calculations were done. First, was the

amount of Cu that could be deposited. Equation 2-3,

$$W = \frac{ItA}{nF},$$ (2-3)

23

where W is the mass of the deposited metal (grams), I is the current (Amperes), t is the

time (seconds), A is the atomic mass of the metal (g/mol), n is the number of valence

electrons (for Cu^{2+}, n=2), and F is Faraday's number (96,485 Coulombs/mol). The

thickness of the particle could be calculated with a known weight and surface area.

Equation 2-4,

$$\delta = \frac{W}{\rho A_s},$$ (2-4)

describes the thickness calculation described above, where δ is thickness (cm), ρ is

density (g/cm³), and A_s is the surface area of the particle (cm²).

Substituting (2-3) into (2-4) to solve for the product of current and time, shown in

Equation 2-5,

$$It = \frac{\delta \rho A_s n F}{A},$$ (2-5)

allows for the simple calculation of either current or time needed to deposit some amount

of Cu onto the W.

Current density plays a big role in the electroplating of copper and a wide range

of current density and throwing power solutions can be used to achieve plating. The

current can be varied within a specific cathode area, in this case the base of a 400 mL

beaker, to achieve a current density that produces good plating results.

In plating in an acid copper bath, like the copper sulfate acid solution used in this

thesis, a relatively low current is sufficient. The current of 0.25 A used in the thesis

experiments, produced at approximately 6 V, produced a cathode current density of

24

0.88 A dm^{-2}. To calculate the plating rate of this experiment type, a few conditions must be known. The cathode area, in the case of this experiment is 28.27 cm^2, or the base area of the cut copper circles that were adhered to the bottom of the beaker to act as the cathode. In a given current cycle, only the top layer of powder was well plated, which corresponded to a surface area that was slightly greater than that of the cathode, due to surface roughness. However, the total surface area of the powder is 10,362.7 cm^2, or 367 times that of the cathode, indicating that of the order of 367 cycles of deposition and stirring are needed to make a uniform coating on 100 grams of W powder. Second, the current must be known, in the case of this thesis, the maximum current of the HY 3003-3 DC power supply is 3A, when connected in parallel. If the maximum current was operated over a period of one minute, the plating rate was 2.34 μm per minute, given these conditions, on the top layer of the settled powder. In the event of a uniformly distributed powder, as described in the first method of standard electroplating in Section 2.3.1, this rate would describe the μm/min for plating on the entire batch. The maximum current produced by the power supply would not be ideal for plating though, as many copper dendrites would grow off the cathode, consuming the copper that was supposed to be deposited on the powder. This would be seen due to a high current density on the cathode and could be diminished by lowering the current. The high current density could also be seen due to a partial coverage of the W particles in oxides, causing a local concentration of current and leading to dendrite production. The dendrite formation can be minimized by eliminating the locally high current density points by removing the oxides from the W particle surfaces. Instead, the current was adjusted to minimize dendrite formation and maximize the deposition onto the W powder. As high current

density depositing with a high throwing power yields great operational cost and productivity benefits. This produces thick coats of copper at a high deposition rate, while producing reduced stress, increased hardness, reduced surface roughness and a lower porosity [2].

2.4.4   Sedimentation Time

The time it takes for the powder particles to settle after being agitated with the magnetic stirring rod can be attributed to a few natural factors. The first, is Stokes' law, which describes the frictional, drag force, that is exerted on sphere shaped object with a small Reynolds number in a viscous fluid. Stokes' law relies on two forces acting on a particle, the drag force and the gravitational force, which are equal and opposite at equilibrium, gravity pulling the sphere down, while drag attempts to prevent it from falling. The terminal velocity of a sphere falling in viscous fluid was determined using Equation 2-6,

$$v_{ts} = \frac{(\rho_p - \rho_f)gD_p{}^2}{18\mu},$$
(2-6)

where g is the gravitational acceleration (m/s^2), D_p is the diameter of the sphere (m), ρ_p is the mass density of the particles (kg/m^3), ρ_f is the mass density of the fluid (kg/m^3), and μ is the dynamic viscosity (kg/m*s). While this method provides an accurate model for the flow of spheres in a viscous fluid, it neglects to address the pressure drag on the particle. The face of the spherical particle is constantly impacted by the solution, slowing down the particle descent, which could have a serious impact on the Reynolds number and remove the particles from the range at which Stokes' law applies. To determine if the

26

force played a significant role, the Reynolds number of this impact was calculated using Equation 2-7,

$$Re_p = \frac{\rho_f v_{ts} D_p}{\mu},$$ (2-7)

this number determines whether Equation 2-6 is a valid assumption because if $Re_p < 0.1$, the viscous forces govern particle movement. V_{ts} was calculated to be 2.24 mm/s, applying this value to Equation 2-7, assuming an average particle diameter of 15 μm, the dynamic viscosity is 1.002 kg/m*s, equivalent to that of water, Re_p was 2.475×10^{-08}, confirming that Stokes' law applies and verifying that Equation 2-6 was permissible to calculate the powder particles terminal velocity [12]. The physical settling time was then derived to be Equation 2-8,

$$Time_{sed} = \frac{Solution\ Height}{v_{ts}},$$ (2-8)

where the solution height was taken from experiment to be 100 mm and v_{ts} was still taken to be 2.24 mm/s, giving a sedimentation time for the powder particles to be about 44.7 seconds. In the actual experiment, the particles take longer to settle, the actual settling time was around twice the calculated number. This was because the copper bar that acted as the anode obstructed the particles above the 30 mm gap and that the time used in this experiment was waiting until particles could no longer be observed in the solution and it became clear blue again. Using this criterion for settling, a full settling time of 100 seconds was allowed in the thesis experiment.

CHAPTER 3

ELECTROLYTIC DEPOSITION

3.1   Purpose

The goal was to create a successful and efficient method for copper plating W powder. Electroplating was selected due to its low cost and efficiency in adhering to conductive materials. Preliminary experiments were performed, isolating different experimental variables, using a macroscopic substrate, to ensure the validity of the solution, the setup, and the procedure. Then, the experiments containing the microscopic W powder were performed to demonstrate the influence that substrate size had on the experiment.

3.2   Experimental Procedures

3.2.1   Electrolyte Solution

The experiment used one of the electrolyte baths described in Section 2.3.1.2. A large batch was made to maintain a constant solution throughout the experiments.

All the ingredients used to create the electrolyte solution were weighed using a Fisher Scientific Education scale or dispensed from a graduated cylinder. The components and their quantities are shown below in Table 3.

Table 3: This table shows the solution composition for a 225mL electrolyte solution for electroplating copper that was used for a single test.

Ingredient	Amount (mL)
Copper Sulfate ($CuSO_4$)	200 mL of 0.1 M (5.02 grams of powder with DI water to reach 200 mL)
Sulfuric Acid (H_2SO_4)	25 mL of 0.5 M
pH	Between 2 and 5

All the ingredients in Table 3 were placed into a beaker and mixed with the magnetic stirring bar. The 2" nylon stirring bar was placed into the beaker and stirred the solution for 30 minutes, when all of the copper sulfate powder residue was dissolved. Once the solution was homogenous, it was stored and sealed in an Erlenmeyer flask, labeled in accordance with Environmental, Health, and Safety (EHS) policies.

3.2.2 Electroplating Experimental Procedure

Metal powder plating experiments were carried out using the methods described in Section 2.3.1. It was estimated that over 367 cycles were needed to encase all the particles of a 100-gram sample, so that they contained 25 % wt. copper. As mentioned, each cycle included three steps.

The first step was stirring. The method of stirring switched between two techniques, depending on the availability of the magnetic stirring drive. The first method, with no ultrasonic bath, used a magnetic stirring rod. The powder particles were vigorously stirred using the magnetic stirring bar at 1100 rpm. The second method, with the bath, used a corded power drill and a polypropylene paddle stirrer. The drill was suspended over the bath and a hole was drilled through the copper anode to facilitate the

stirring of the solution. These methods allowed the particles to be uniformly suspended in the solution and fall randomly back to the cathode so that new particles may be plated. They were intended to break up any copper bridges that may have formed in the previous plating cycle. This method also reduces the concentration gradient of copper ions in the electrolyte bath that were formed by high-current electroplating.

The second step is sedimentation. The stirring is stopped, and the particles can settle back on the cathode. Sedimentation time for this experiment is calculated using Equation 2-8, in Section 2.4.4. After sedimentation, the newly exposed particles can be plated. A secondary effect of this step is that the loosely settled particles create channels that allow the electrolyte solution to spread to particles below the top surface of the powder. This allows for a small amount of copper to deposit on particles that are below the surface layer, slightly increasing the deposition area.

The final step of the cycle is electroplating. Once the particles have settled onto the cathode, a direct electric current is passed between the anode and cathode, reducing copper from ions in solution onto the powder for 60 seconds. After that time, the current is stopped, and the cycle begins again.

3.2.3   Analysis Procedure

To view the effectiveness of the electroplating experiments, energy dispersive x-ray spectroscopy (EDS) and back-scattered electron (BSE) techniques were utilized. The SEM allowed for the determination of the average W particle size range. In the preliminary test for control analysis, the W powder was placed into the SEM without any solution interaction or plating. The samples were analyzed using a Zeiss Evo 50 scanning

www.manaraa.com

electron microscope (SEM), with back-scattered electron imaging. An image of this is

shown below in Figure 8.
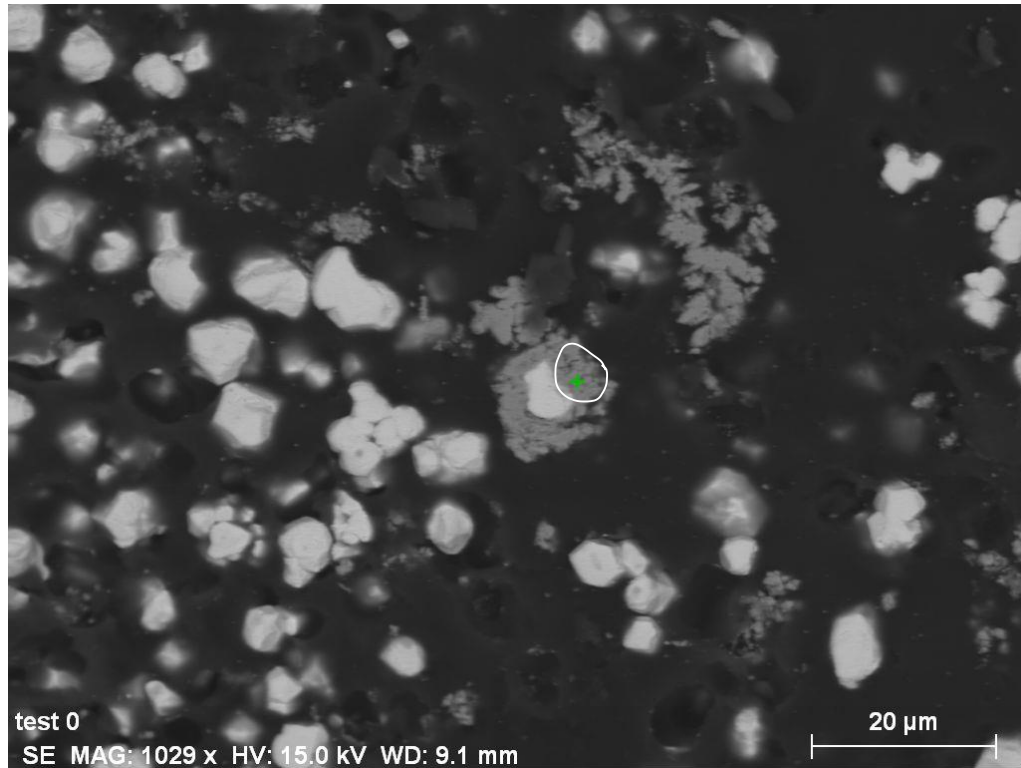
Figure 8: W particles (white) with copper (gray) in the powder. Taken using an SEM, with 20 μm scale bar for reference to particle size. The plus sign discussed in the text is circled in the figure.

Once in the SEM, the sample was magnified, the BSE images were used to

determine the plating thicknesses and an image was captured so EDS analysis could be

done on the particulates, to determine the elemental composition of the powder. A sample

EDS plot was shown in Section 2.2.2, and another is pictured below in Figure 9 showing

peaks of Cu and W. The y-axis of the EDS plot shows the number of counts taken per

second over a one-minute period and the x-axis represents the energy level for those

counts. Various peaks present on the graph labeled W and Cu represent the different x-

31

ray phases, they are labeled with colored lines of uniform height to show the expected

wavelengths of the peaks for Cu and W. W is a heavier element, which means that it has

more electron orbitals, providing more opportunities to excite different transitions, in

turn, leading to W being defined by higher order x-rays. The largest peak of the W

represents the M-α series x-rays, the leading W peak represents the M-ζ x-rays and as the

energy levels get larger, the L-series x-rays are represented by smaller peaks, and the L-

series x-rays are used to define the composition of the elements present in solution, that

are referred to in Section 2.2.2.
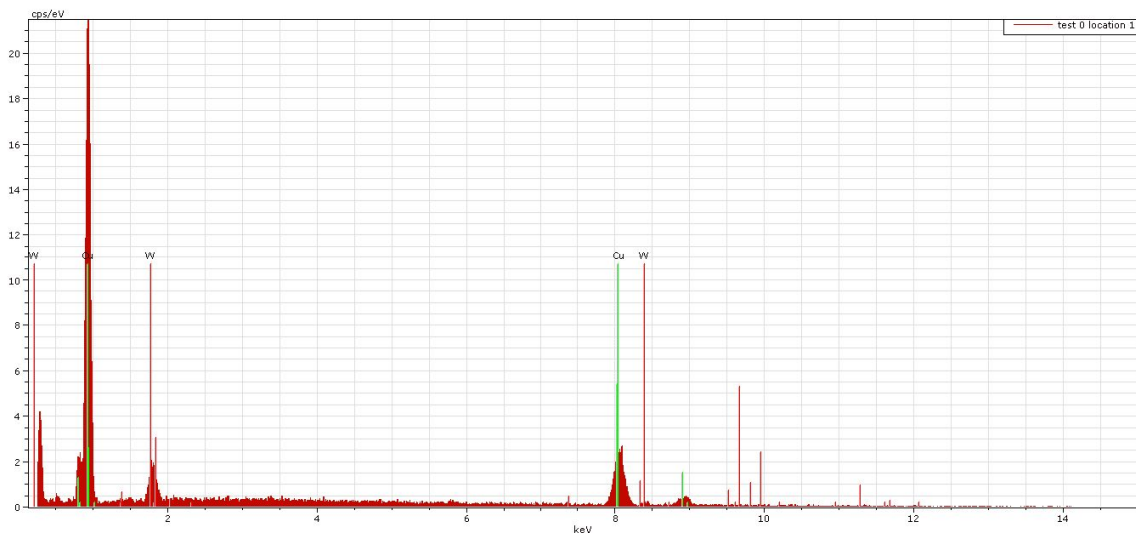
Figure 9: This EDS plot is for the image in Figure 11. The data was retrieved where the plus sign is in mostly darker material, indicating a lower atomic mass, so it is expected that copper would be prominent, however, based on Figure 6 and 7, it was expected to see trace amounts of W in an area like this. These expectations are confirmed in the graph, with a small peak at W Mα x-rays.

A BSE detector was used to determine the difference between the elements

present in the powder. Figure 10 shows a BSE image of the Cu and W, with a marked

difference in contrast between the two elements. Electrons generate a range of collisions,

both elastic and inelastic, with the substrate. The BSE detector harnesses the

backscattered electrons and obtains a response based on trajectory changes during elastic

32

collisions. Larger atoms have larger cross-sectional areas, leading to a higher probability of elastic collisions. Therefore, larger atoms will have more backscattered electrons returning to the detector, leading to a higher intensity, or brighter, sample than lower areas, which appear darker. With this, it comes as no surprise that the W in Figure 10 is much brighter than the Cu.

The cloudy region discussed in Section 2.2.2 and displayed in Figure 6, leads to caution when analyzing BSE images with EDS, as there may be W present under the Cu seen in Figure 10. This volume overlap could potentially lead to errors in the EDS plots causing a Cu coating to show traces of W because it is present underneath the cross-sectional area that is presented. It can be noted that if trace amount of W appears in an EDS reading, where the cross section is clearly Cu, the W counts can be considered negligible and that it is due to the volume overlay, rather than it actually being present in the particular cross section.
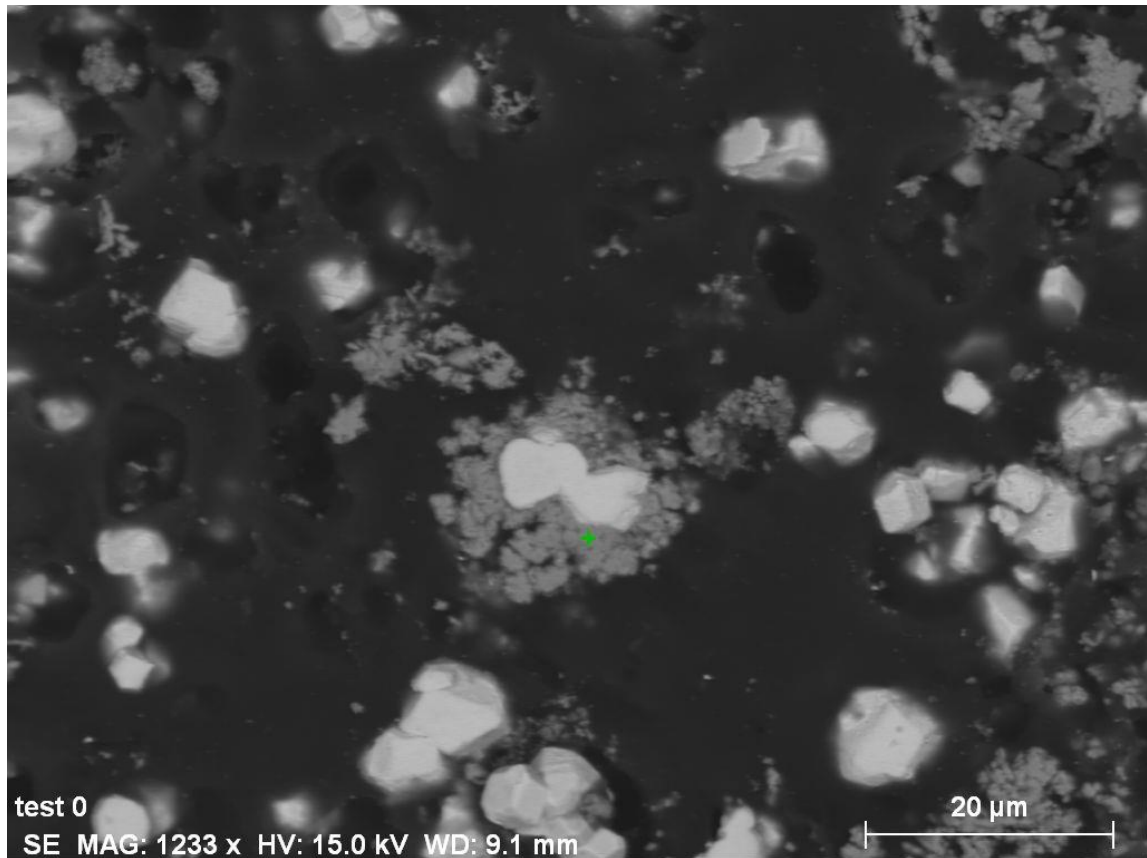
Figure 10: This figure displays the point that the EDS results in Figure Y were analyzed from, denoted by the plus sign. The region is slightly into what is now defined as copper, so it was expected that we would see trace amounts of W, especially so close to the brighter W particles. This expectation is a result of the cloudy region surrounding the particles. This effect can be seen in some of the surrounding particles, however, Figure 5 provides a better look into the exact areas denoted as cloudy.

3.3   Preliminary Procedures

All the glassware was cleaned and prepared in accordance with the procedure shown in Appendix C.

3.4 Macroscopic Substrate

3.4.1 Overview

For the nickel coin and tungsten foil substrates, no stirring was used, and the electroplating setup contained no ultrasonic bath. These tests were designed to provide clear tests about electroplating with the apparatus onto a familiar substrate, and then onto tungsten. They were used to provide essential results regarding the current density, sample thickness, the effect of varying pretreatments, and verification of the appropriateness of the electrolyte bath.

3.4.2 Equipment

For the macroscopic substrate tests, the cathode was made of copper foil that covered the bottom of the beaker with a thin tail that was fed up the side of the beaker, to allow contact with the negative power supply lead. The anode used for these experiments was a 2" diameter copper rod, connected to the positive power supply lead. No magnetic stirring was used in the macroscopic experiments.

3.4.3 Setup

To visualize the electroplating apparatus used in this experiment, Figure 11 below, gives a breakdown of the setup and the general concept behind the electroplating mechanism used. For the macroscopic substrate, no stirring bar was used, but the remainder of the setup is consistent. Current is applied by a DC power supply connected in parallel, producing a current of approximately 0.25 A through the solution. The copper rod anode was mounted to a ring stand with a clamp attachment to hold the rod in place. For the macroscopic substrate and initial powder testing, the beaker was placed on top of the magnetic stirring pedestal, but magnetic stirring was only used in the microscopic

35

testing. Note that in Figure 11, the copper foil tape cathode has a contact strip that extends out of the beaker, this contact was insulated from reacting with the anode before the cathode using a polypropylene tube [11]. This contract strip method was developed by Rigali in order to plate powders in a beaker and it played an integral role in achieving a working apparatus.

After the initial electroplating that was described above, the resultant powder was filtered using a vacuum-assisted filter to remove the electrolyte solution and begin the drying process. Then, the powder was left for an hour in a vacuum desiccator to remove excess moisture that remained. This process is further outlined in Appendix A.
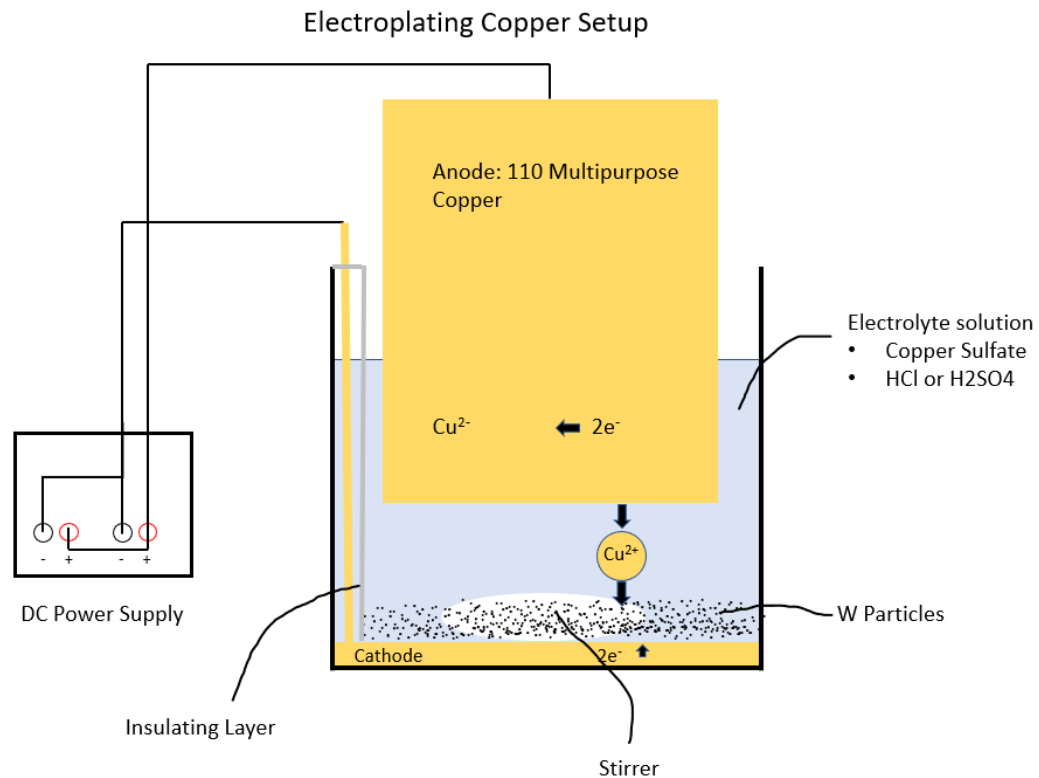
Figure 11: Electroplating of copper setup. The DC power supply is linked in parallel to supply the necessary direct current through the electrolyte solution. The copper ions are depleted at the cathode and replaced at the anode. Electrons available at the cathode attract the positively charged copper ions, transforming them into copper metal upon contact with the cathode surface.

3.4.4 Procedure

Both macroscopic substrates, the coin and the W foil had the same electroplating procedure, although the W foil had extra pretreatments, including a nitric acid wash or a hydrofluoric acid etch, outlined in Appendix B. The substrates were placed on top of the cathode and the anode was lowered over them to create a 30 mm separation. A direct current of approximately 0.25 A was then constantly applied for two hours to each of the substrates. This current corresponded to an ideal current density for the acid copper baths [2].

It was found that 0.25 A was a sufficient current that created enough overpotential to achieve a current density in the ideal range for an acid copper bath, but did not provide an excessive amount, which would have led to the creation of hydrogen bubbles in the solution if the copper ions became exhausted from the boundary layer at the cathode. Accordingly, a current of 0.25 A was used throughout the macroscopic and later microscopic experiments.

3.4.5 Results and Discussion

Using the thickness calculation presented in Section 2.4.2, the thickness coating on a coin and W foil was able to be approximated under the assumption that the deposition was 100% efficient. Figure 12 displays a backscattered electron image of one of the coins that was electroplated for approximately two hours in the HCl electrolyte bath. Using the maximum plating thickness displayed in Figure 12, 15.12 μm, Table 4 was constructed to display the theoretical calculation and the observed values of plating thickness.

37
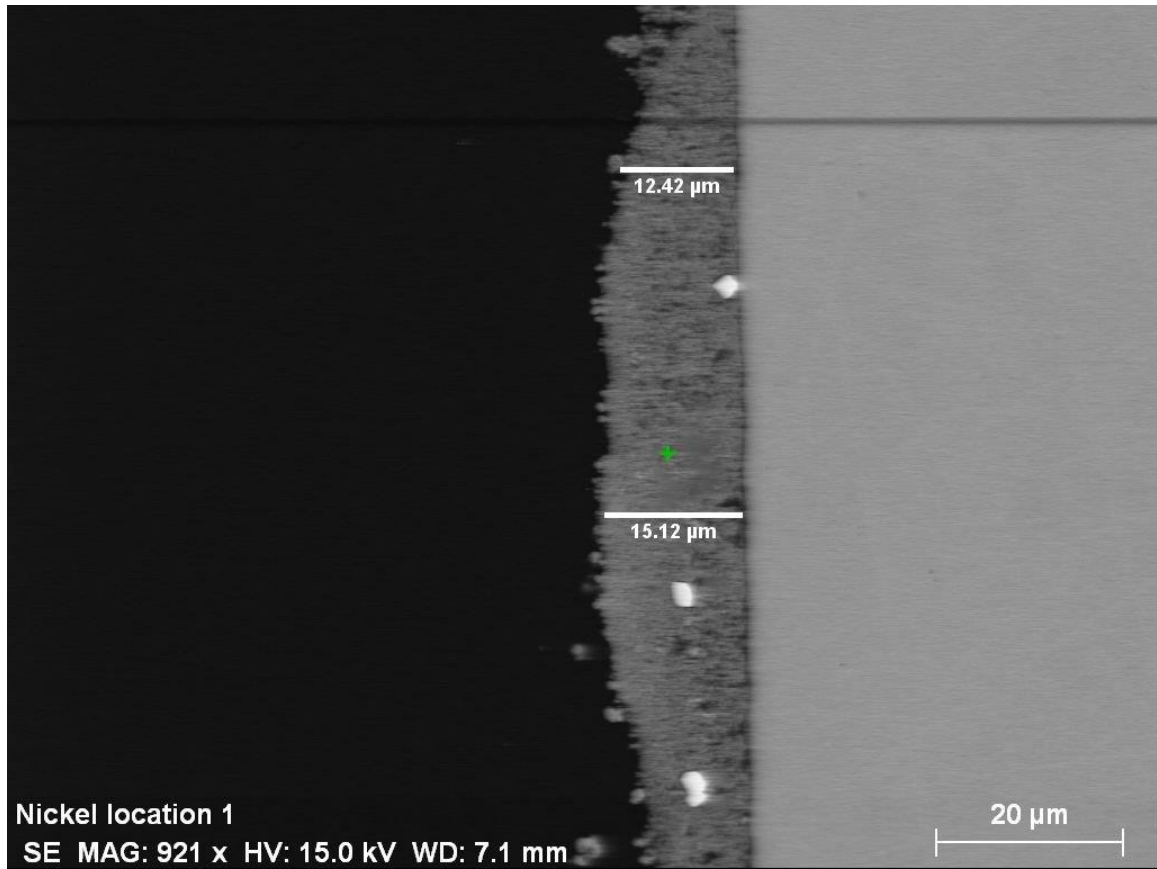
Figure 12: This figure depicts the variable thicknesses of copper plated on a nickel coin for approximately 2 hours.

Table 4: This table illustrates the calculated and observed thicknesses for the nickel coin plated in copper that is shown in Figure 9.

Nickel Plating Thickness	Calculated	Observed	Efficiency
Thickness (um/min)	0.20	N/A	N/A
Thickness (um/2 hr)	23.40	15.12	65%

In Figure 12, the contrast between the copper and nickel coin is very distinct, the coin is the smooth surface, while the copper is the darker, more variable surface. This contrast allowed for the simple measurement of plating thickness, shown on the figure to be 15.12 μm. The thickness is visibly not constant along the nickel surface, with a second thickness value being displayed on the figure. The thickness along the boundary is

38

slightly variable, but there are no areas where the coin was drastically different from the others.

Table 4 depicts the calculated thickness values that were expected on a nickel coin after 2 hours. Note that the actual value is slightly lower than the expected due to copper losses to the cathode during plating, so the efficiency was only 65%. The rate of deposition during the experiment was not constant, which can be credited to the extra plating onto the cathode. Figure 13 illustrates the deposition of copper onto the cathode with small dendrites forming on the top during the electrolytic deposition during a macroscopic substrate test, in this case W foil, but the nickel coins had the same results.
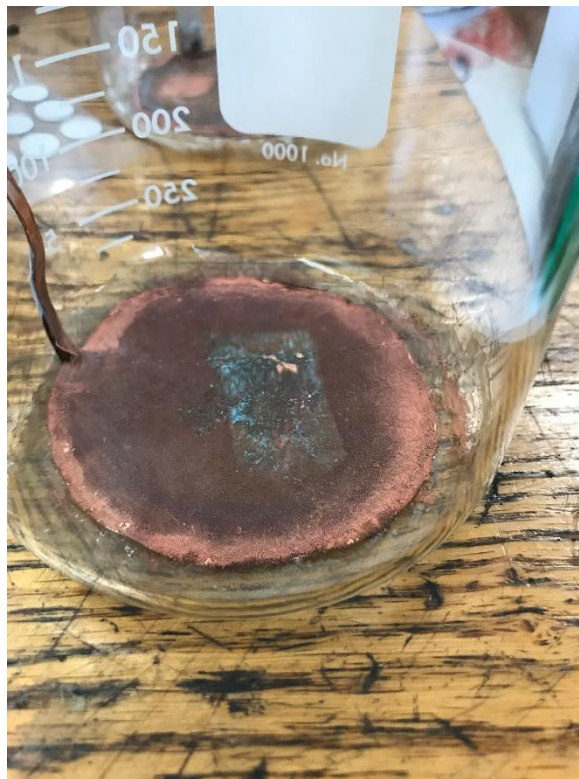
Figure 13: This figure depicts copper deposition and dendritic growth on the cathode, while showing the shadow of where the HF pretreated foil was during the deposition.

The shadow towards the center of the cathode is the place where the HF

pretreated foil rested, other tests had similar imprints for W foil and nickel pieces. The

main takeaway is the copper deposition onto the cathode. Dendrite growth can be seen on

the cathode away from the foil spot, showing that some of the copper was consumed by

the dendrites instead of the nickel or W foil, leading to the lower efficiency value. Figure

14 provides a second example of a post experiment beaker that highlights the foil

imprints for a test of the other foil types.

Figure 14: Experimental beaker after a foil test with a nitric acid, abrasion, and no pretreatment foil test. Note the prominent shadows left on the cathode where the foil was.

Figure 14 displays the discussed shadows from the macroscopic substrates more clearly. In this experiment, 3 types of pretreatment for the W foil were tested, a nitric acid pretreatment, an abrasion pretreatment, and no pretreatment.

The electrolyte bath in the foil tests was the H_2SO_4 bath, as the initial powder tests conducted ruled out the use of an HCl bath. The results of the HCl bath are presented in Sections 3.5 and 3.6. The W foil test was created to be a macroscopic experiment that closely related to the powder experiment due to the use of the same element. However, that flat foil surface allows for less difficulty in plating. The experiment entailed testing three pretreatment options and a control with no pretreatment. The three pretreatments were a nitric acid wash [11], a hydrofluoric acid etch [13], and a Scotch Brite abrasion. The acid pretreatments are outlined in Appendix B, and the Scotch Brite abrasion was simply using a Scotch Brite steel wool pad and scraping the dry surface in hopes of removing the surface oxides from the foil, and to create a rougher surface to test the effect of plating onto a rougher surface.

The procedure itself remained the same as the nickel coin procedure after the pretreatments. The foil test provided a look into how the W powder plating feasibility would be with each of the pretreatments. Figure 15 shows the foil results for all the tests, except the HF etch, in the form of a BSE image.
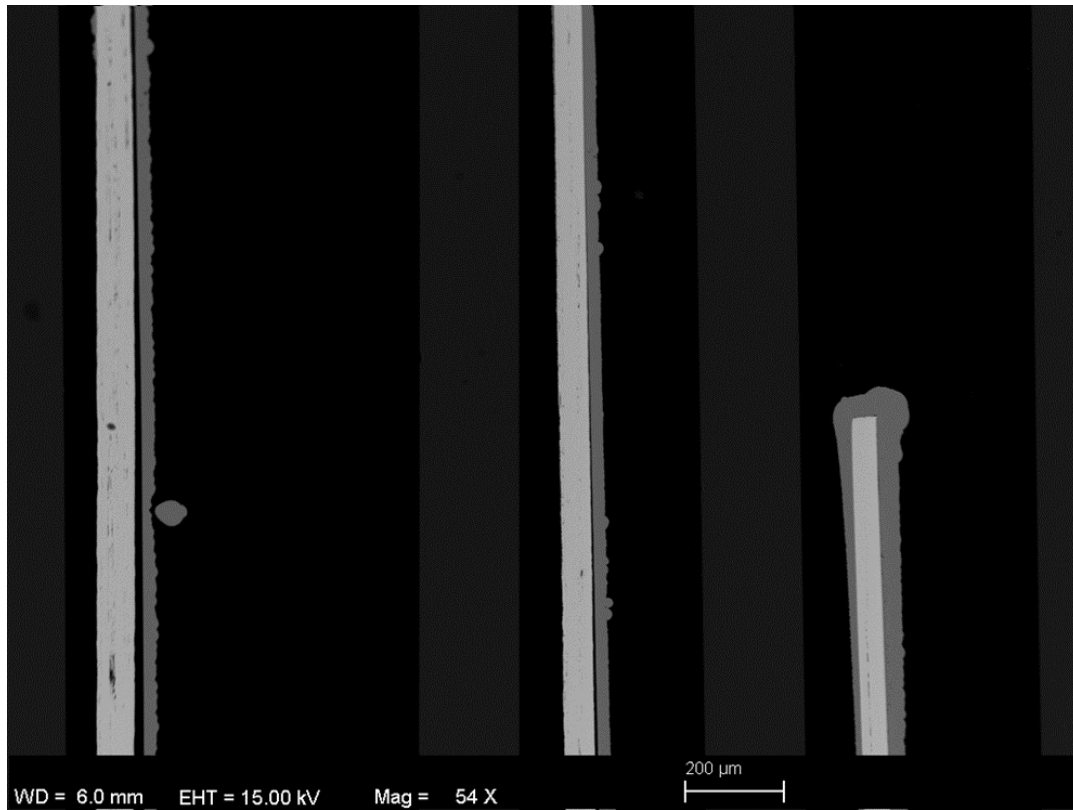
Figure 15: This figure depicts plating results for, from left to right, a nitric acid wash, a Scotch Brite abrasion, and no pretreatments.

Of these three tests shown above, the no pretreatment showed the best results. The W foil with no pretreatment showed a good connection to the foil, adhering to the surface better than the other two pretreatments that appeared to pull away from the foil. The lack is bonding to the foil in the two pretreatment methods shown is suspected to be due to an oxide layer on the surface of the W foil. The foil that was not pretreated did show some porosity at the boundary, indicating the presence of the same condition, but not to the same extent. Figure 16 shows the W foil pretreated with an HF electro-etch, demonstrating no gap.

42
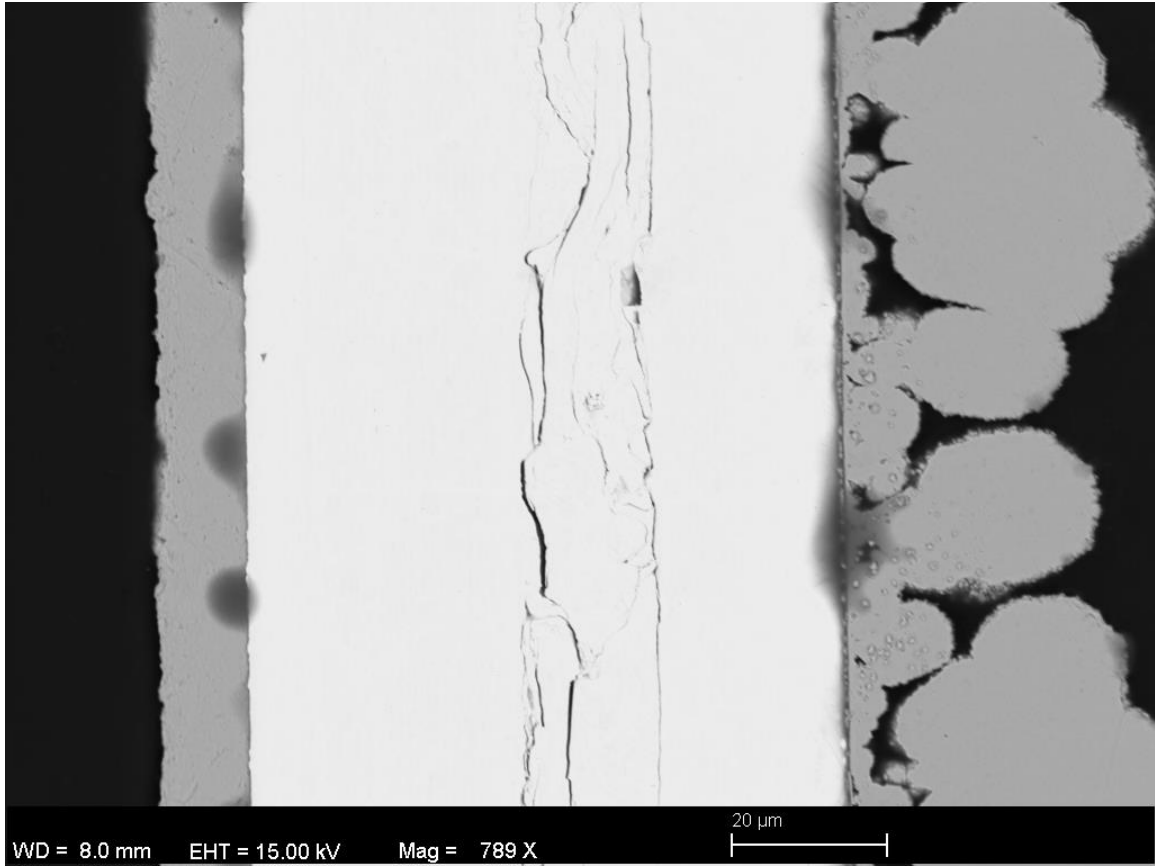
Figure 16: HF electro-etch pretreated foil, shows minor porosity at boundary, but good bonding to the surface of the foil.

In the test shown in Figure 16, half of the foil was dipped into the HF solution for etching and the other half was not, acting as another no pretreatment test. This no pretreatment test yielded similar results to those of the Scotch Brite and nitric acid wash pretreatments, showing some separation at the boundary, this result is shown in Figure 17.

43
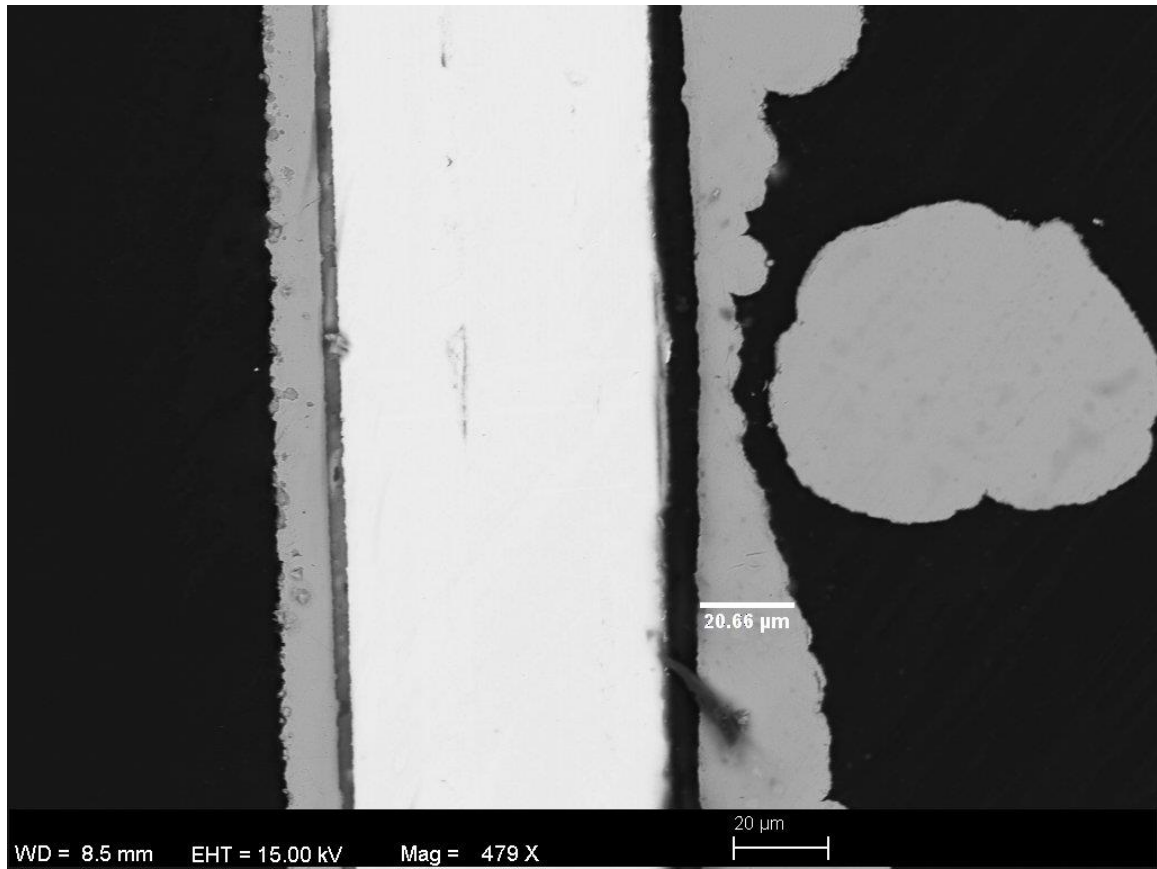
Figure 17: This figure depicts part of the foil that was not pretreated to maintain a control during the HF electro-etch test.

The foil test also provided validation of the thickness calculation, as each of the substrates was left in the electrolyte solution under direct current for two hours. Each yielded a plating thickness of around 20 μm. Refer to Figure 17 to see a sample of the plating thickness, measured using ImageJ. This thickness was taken as an approximation, as the sample had variable thickness. The compiled thickness values for the 5 foil tests, including the control, no pretreatment, from the HF test, and their efficiencies, given their deposition time, are displayed below in Table 5. This test resulted in the further experimentation with an HF electro-etch pretreatment for the powder, presented in Section 3.7.

44

Table 5: This table presents the plating thicknesses and efficiencies for all the foil test with their respective pretreatments

Foil Plating Thickness			
Pretreatment	Calculated (um)	Observed (um)	Efficiency
No Pretreatment (original)	23.40	19.34	83%
Scotch Brite Abrasion	23.40	21.33	91%
Nitric Acid Wash	23.40	19.76	84%
HF Electro-Etch	23.40	20.97	90%
No Pretreatment (HF control)	23.40	20.66	88%

Although the efficiency of plating for the HF electro-etch was not the best, all the efficiencies were comparable. In addition to having a high efficiency, the HF etch provided the best bonding to the surface out of all the foil tests, leading to experimentation with the HF electro-etch pretreatment process with the W powder. The 0.25A current that corresponded to a current density of 0.88 A/dm^2 was determined to provide sufficient bonding with fewer dendrites forming on the cathode than at higher current densities. This allowed for the reduction of copper "loss" to the foil cathode.

3.5   W Powder No Pretreatment

3.5.1   Overview

This collection of powder experiments was conducted to test plating of the powder with no pretreatment as a control case. These experiments allowed for the analysis of the effects of current density, electrolyte solution and the initial bonding tendencies at the W and Cu boundary.

3.5.2   Procedure

The apparatus used was that pictured in Figure 11. The powder experiments did use the magnetic stir bar to mix the powder into the electrolyte solution. The stirring was

done at 1100 rpm for 20 seconds. The powder was then allowed 100 seconds to settle

back to the cathode before current was applied. The direct current between the anode and

cathode was then applied for 60 seconds, so that copper ions could be deposited onto the

powder surface. A different current was used in different tests, from 0.25 A up to 2.5 A.

This cycle was repeated 20 times for each of the no pretreatment experiments. Once the

cycles were complete, the powder was filtered in accordance with Appendix A. The dry

powder sample was then mounted in an epoxy puck to initialize the SEM preparation.

The sample was then ground and polished to reveal a cross-sectional view of the particle.

After the post-electroplating preparation was complete, the samples were ready to

analyze in the SEM.

3.5.3   Results and Discussion

All the images were evaluated in the same way, BSE imaging with a 20 μm scale.

Figure 18 depicts a powder test conducted at a lower direct current. The figure shows a

lot of copper agglomeration and an extremely limited amount of bonding to the W

powder surface. The copper agglomeration itself appears in dendritic form, indicating

that it may have grown from the cathode at a high local current density spot. Copper

deposits where the electrolyte solution meets electrons. A bare metal surface would be

plated uniformly for a moderate current density. A surface coated in non-conductive

oxide would be plated only at gaps in the oxide coating. Subsequent deposition would

occur only on the newly deposited copper, resulting in this high local current density,

causing the dendrite morphology to occur. The current in the figure is 0.6 A and

corresponds to a current density of 2.12 A/dm^2. This lies within the ideal range for

plating in an acid copper bath, in this case, the H_2SO_4 version, however, no plating is

visible, indicating that something is barring the copper from depositing on the surface. Given this, it was hypothesized that there was an oxide layer on the W powder preventing the conduction of current to the surface.
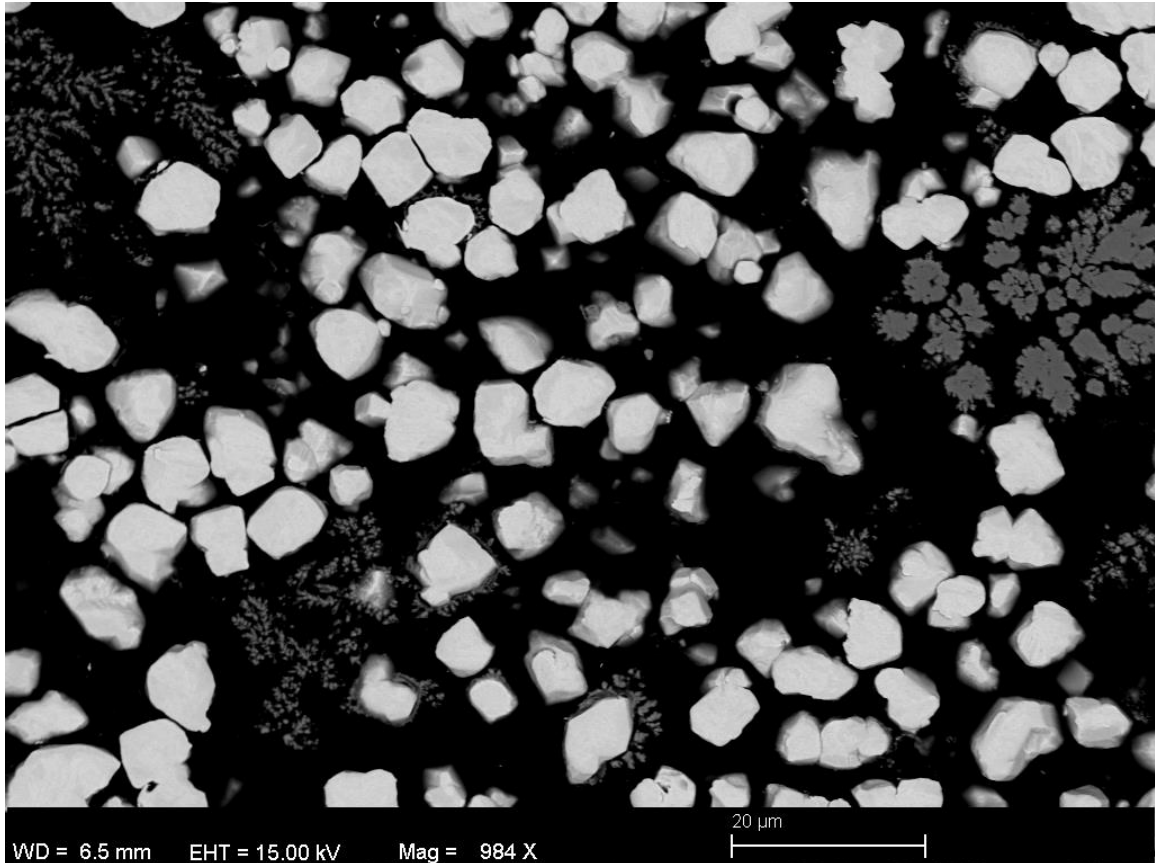
Figure 18: This figure depicts the W powder without a pretreatment at a current of 0.6 A

With the results after 20 cycles at a low current showing no plating, a higher current was used. At a higher current, it appeared that some plating was taking place on the non-pretreated particles, however, there was a significant amount of dendritic growth from the plated particles, as well as a separation at the W-Cu interface.

47

Figure 19 shows the non-pretreated W powder after a direct current of 1.0 A in an H2SO4 bath for 20 cycles. The separation that was discussed is a small dark ring surrounding the white particles before the dendritic copper begins.

WD = 7.0 mm   EHT = 15.00 kV   Mag = 701 X   20 µm
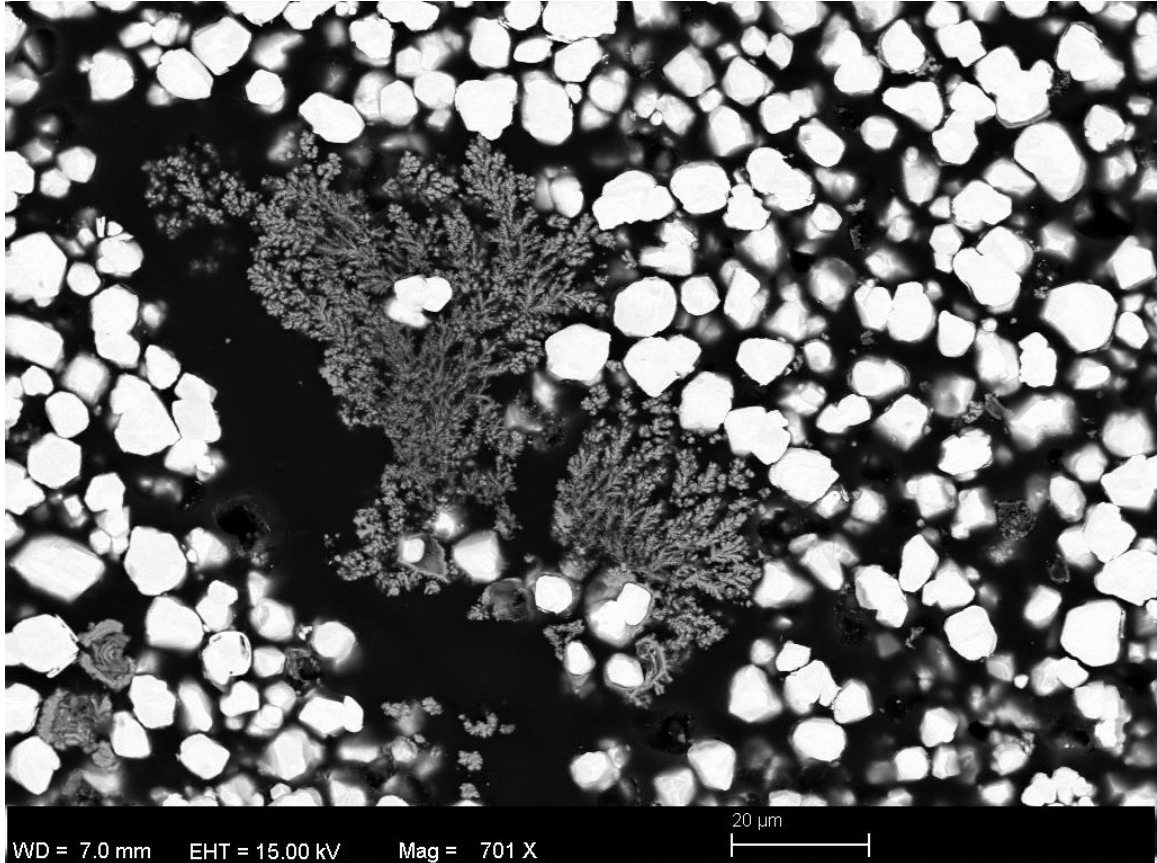
Figure 19: Non-pretreated powder with a direct current of 1A applied through the electrolyte bath

As the current got higher, the growth of the dendrites became more severe, indicating that these particles were areas of locally high current density and that the plating was focused on adding to the dendrites instead of the particles. This test provided further evidence to move forward with an acid wash to try and take the presumed oxide layer off the powder. At the upper bound current density from [2] of 10 A/dm^2, the

48

dendrite formation was not visible anymore. Instead, the copper deposits began to form

vast clumps and show no signs of successful plating, but rather, entrapment by copper

agglomeration. Figure 20 displays the recommended upper bound for current density,

given the cathode area, or 3A in an HCl electrolyte bath.
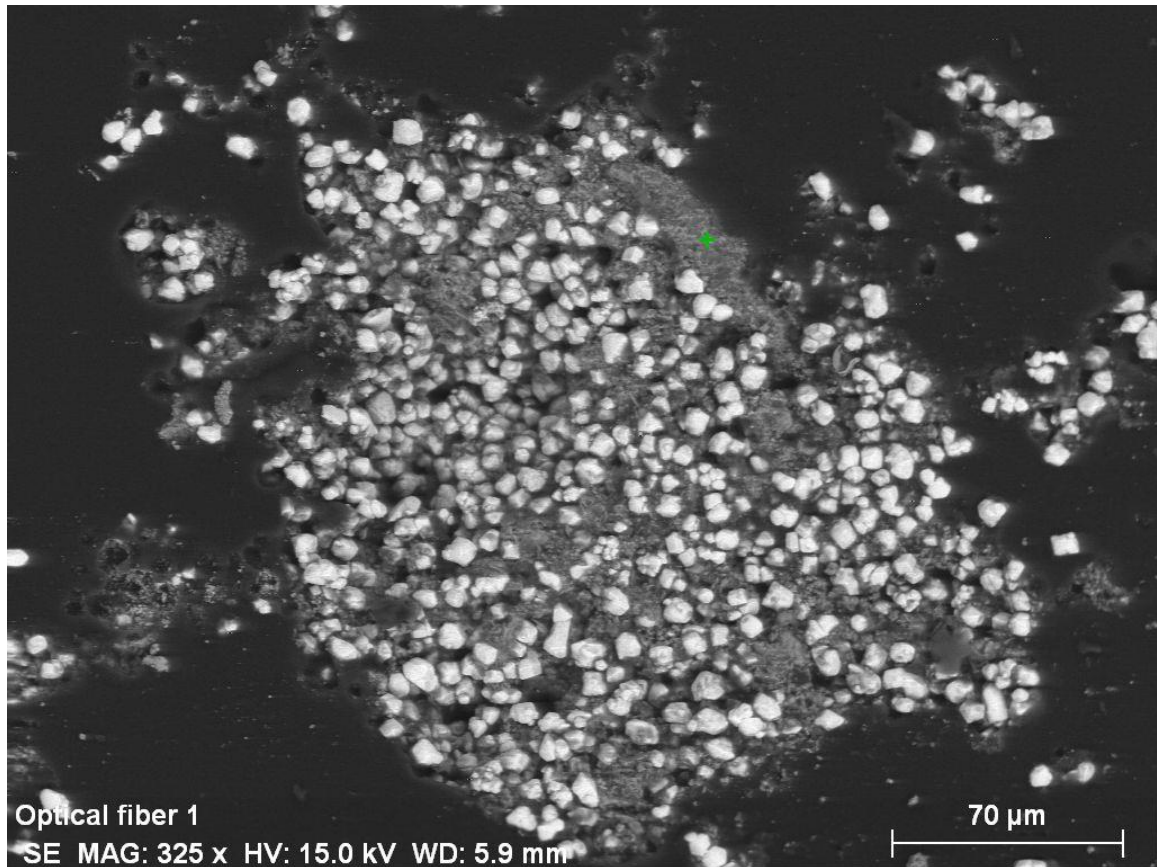
Figure 20: Non-pretreated powder with a direct current of 3A applied through the electrolyte bath

The clustered nature of the particles indicated the current density was too high

and the copper was growing off itself and trapping the particles, rather than plating on

them. In general, if the particles remained unpretreated, successful plating would not be

plausible, leading to a nitric acid pretreatment to attempt to rid the particles of the

49

presumed oxide layer. However, the results from the non-pretreated particles demonstrated that a lower current density had a better chance at visibly adhering to the W particles.

3.6 W Powder with Nitric Acid Pretreatment

3.6.1 Overview

These powder experiments were conducted to assess the effectiveness of a nitric acid pretreatment on the W powder to remove the surface oxide. The experiments allowed for the analysis of the effects of current density, electrolyte solution and the bonding tendencies at the W and Cu boundary for this pretreatment.

3.6.2 Procedure

Refer to Section 3.5.2, as the procedure used for these two experiment types were the same. However, this experiment did have a pretreatment process that is outlined in Appendix B. This process is like that presented in [8], which has obtained successful results in encasing W particles in copper.

3.6.3 Results and Discussion

The nitric acid pretreatment tests yielded similar results to those of the no pretreatment, however, there were cases of bonding between the W particles and the copper. Largely, the nitric acid wash produced the same cluster of particles at higher current densities and showed some plating, although fewer dendrites, than the powder that was not pretreated. Figure 21 shows a nitric acid pretreatment that was run at the upper bound of the current density in the HCl electrolyte solution.

50
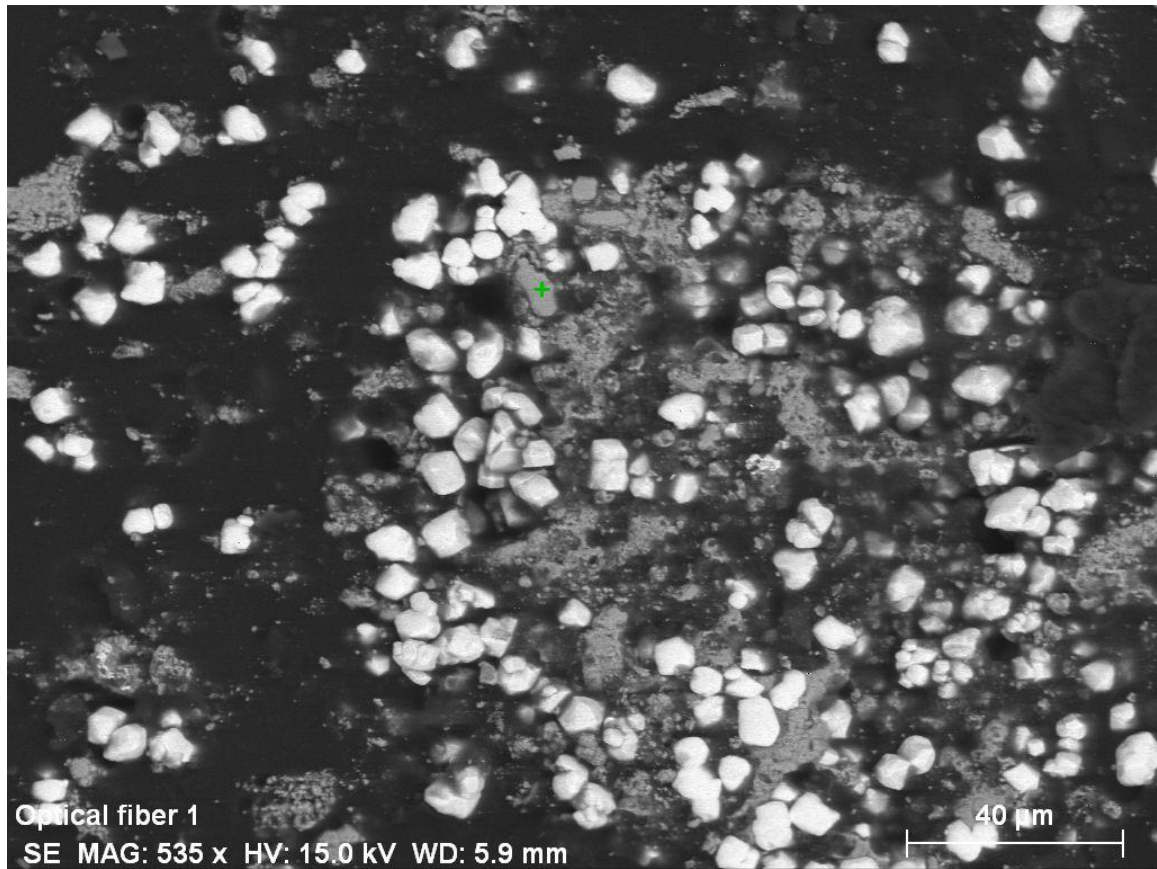
Figure 21: This figure depicts a high current, 3A, being passed between the anode and cathode, after a nitric acid pretreatment

Figure 21 exhibits clustering, like that of the non-pretreated powder, however, clusters are not as drastic. From these results, it was possible that the high current density was causing extremely high local current densities in places that had limited surface oxides and that the nitric acid wash did not remove the surface oxide layer as anticipated, accounting for the massive amount of agglomeration and limited plating. There are traces of bonding between the copper and W powder, however, these connections could be due to gaps in the oxide layer, rather than actual surface cleaning, as was seen in the non-pretreated powder. While it is a step closer to the goal of encapsulating the W particles, the nitric acid wash was not effective at this current density. The absence of dendrites

51

was consistent with the results from the non-pretreated powder at the high current

density. However, unlike the non-pretreated powder, a deeper analysis of the powder

sample revealed some particles containing sufficient bonding between the W and Cu,

shown in Figure 22.
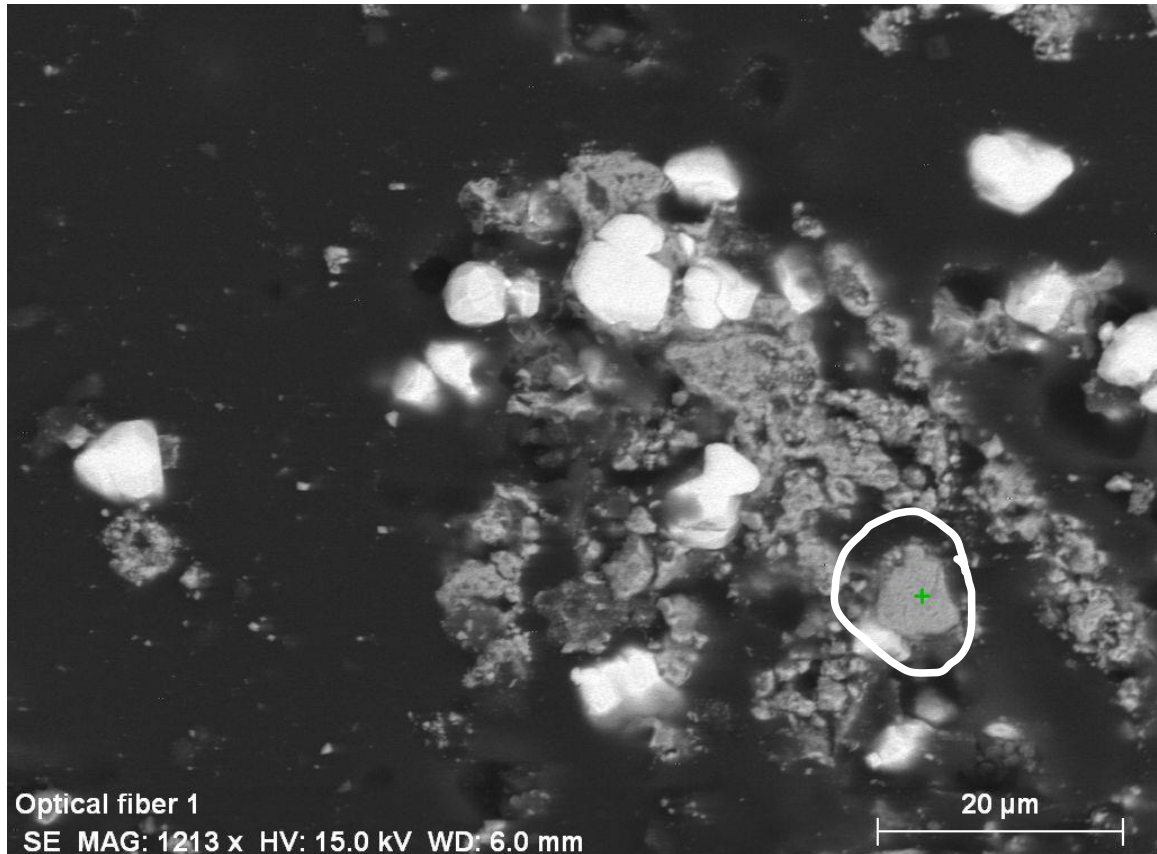
Figure 22: Nitric acid pretreatment at high current showing copper adhering to W surface. Particle shaped agglomeration is circled in bottom right

Figure 22 depicts that the high current density allowed for plating into the obscure

geometries of the particles, but the coating itself was not uniform and contained a very

uneven surface, if the plating was successful. Once again, it looked to be a result of

plating in an oxide layer gap, then having copper ions being attracted there due to its high

52

local current density. This is supported by excess of copper surrounding the W particles and only adhering to the particle in a few areas.

Another indication that some plating may be occurring is the circled, particle-shaped, agglomeration in the bottom right corner. Spots like this occurred in various places throughout the sample. Where this could be a coincidental agglomeration of copper, it could also be the flat side of a coated W particle. It is not evidence of successful plating, but rather another instance to look for in SEM analysis that if paired with a successful plating could be determined to be a plated particle rather than a particle shaped agglomeration.

With the nitric acid pretreatment providing somewhat unsuccessful results for plating, unlike those shown in [8], further research was conducted to devise a new step forward. A patent described an HF electro-etch pretreatment for removing the oxide layer from the surface of W before electroplating [13], which was adapted for the next set of experiments shown in Section 3.7.

3.7   W Powder with HF Electro-Etch Pretreatment

3.7.1   Overview

The HF electro-etched powder experiments used an ultrasonic bath and implemented the corded power drill and a mixing paddle for stirring. These experiments were designed to compile the favorable results from the other experiments and add in ultrasonic agitation. These experiments contained a constructive current density, electrolyte bath and the implementation of the most promising pretreatment for the powder. They were used to verify the powder pretreatment and the ability of the copper

to adhere to the powder given the compilation of the best components from the other experiments.

3.7.2   Procedure

The procedure for this method was like the previous powder procedures, except for the fact that the beaker containing the powder during plating was in an ultrasonic bath, which was turned on for the duration of the experiment to ensure constant agitation of the particles. The setup itself was the same as that in Figure 11, except the beaker was specifically high-density polyethylene (HDPE), so it does not react with the HF, but that beaker lies in a bath, as demonstrated in Figure 23. As seen, the stirring mechanism changes from a magnetic stirring rod to a corded drill and polypropylene paddle stirrer, and instead of a copper rod, an end fitting with a hole milled in the center replaced it.

Figure 23: HF pretreatment test setup

The HDPE bin seen next to the ultrasonic bath was the area in which the HF

electro-etch took place, per the procedure in Appendix B. This electro-etch was primarily

reliant on the Pourbaix diagram presented in the patent, Figure 24 [13]. This figure shows

the conditions that should allow removal of the oxide from the W powder without

producing hydrogen. The key region of the diagram is Region "C", as when the voltage
and pH are in this region, the etch is predicted to reduce the oxide..

FIG. 4 POURBAIX DIAGRAM OF W ILLUSTRATING REGION
WHERE W IS OXIDE FREE
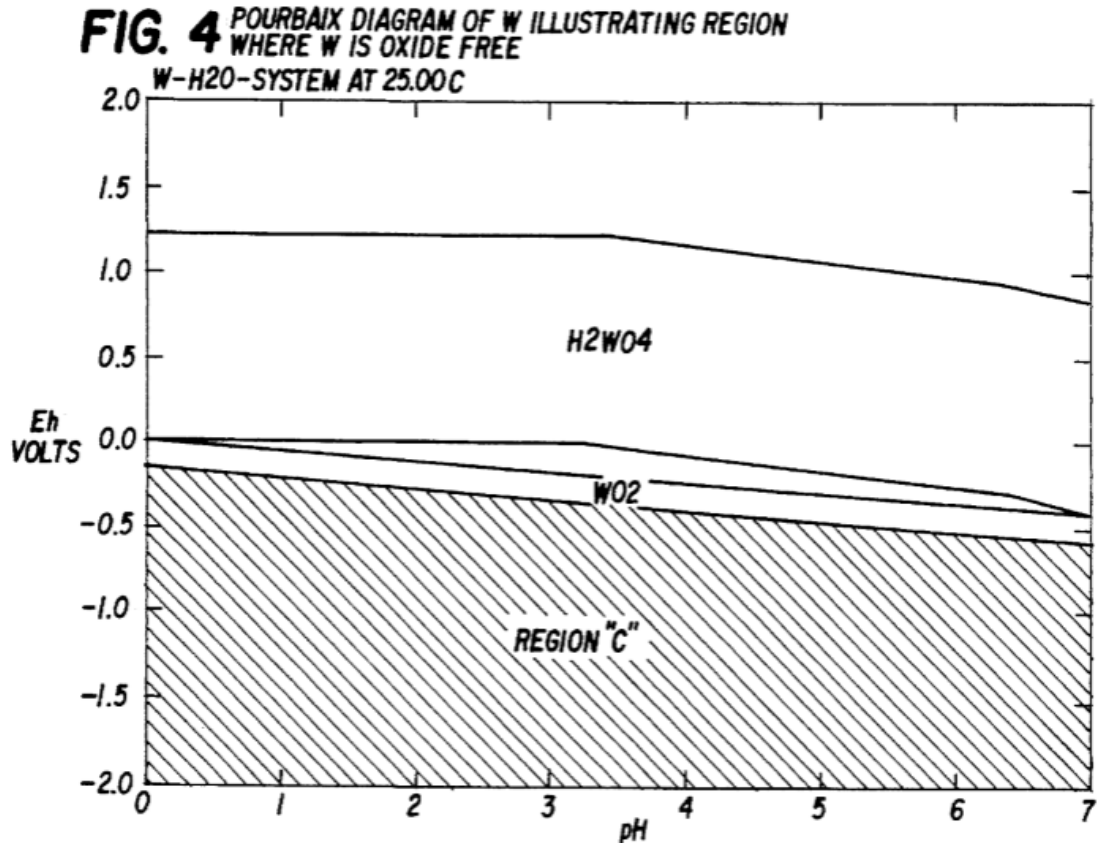
**Figure 24: This figure depicts the Pourbaix diagram from the patent for the HF
electro-etch [13]. Keeping the voltage potential within Region "C" will allow for the
W powder oxide layer to be removed without producing hydrogen.**

Once the electro-etch was complete, the connections were terminated, and the
etch solution decanted by pouring the HF solution into a second HDPE beaker and
retaining most of the powder in the original. Then, the electrolyte solution was poured
into the original HDPE beaker with the powder and placed into the ultrasonic bath. The
drill mechanism was lowered down so the paddle could stir the powder and the copper
end fitting was held in place just above the end of the paddle. The ultrasonic bath was
turned on for the duration of the experiment, then the same plating cycles from Section

56

3.5.2 were employed, but more than 20 steps were used. As mentioned, to plate all the powder in a 100-gram batch, it would take at least 367 steps. That experiment would take over a day to run, so a repeat cycle timer was implemented. For this HF pretreatment experiment, a two-hour duration was used, with the repeat cycle timer, to obtain results without sacrificing time.

3.7.2.1 Repeat Cycle Timer

A repeat cycle timer was created using an Arduino compatible, Elegoo Uno, a packaged microcontroller, to automate the cycling process. The timer was connected to an AC/DC relay and switch board, along with a dual-input, 120V outlet. A picture of the repeat cycle timer is shown in Figure 25. The timer allows two inputs to independently be turned on and off for a set amount of time, in this case, the DC power supply and the corded drill. The timer was successful in completing a 24-hour trial run to prove its ability to complete an experiment.
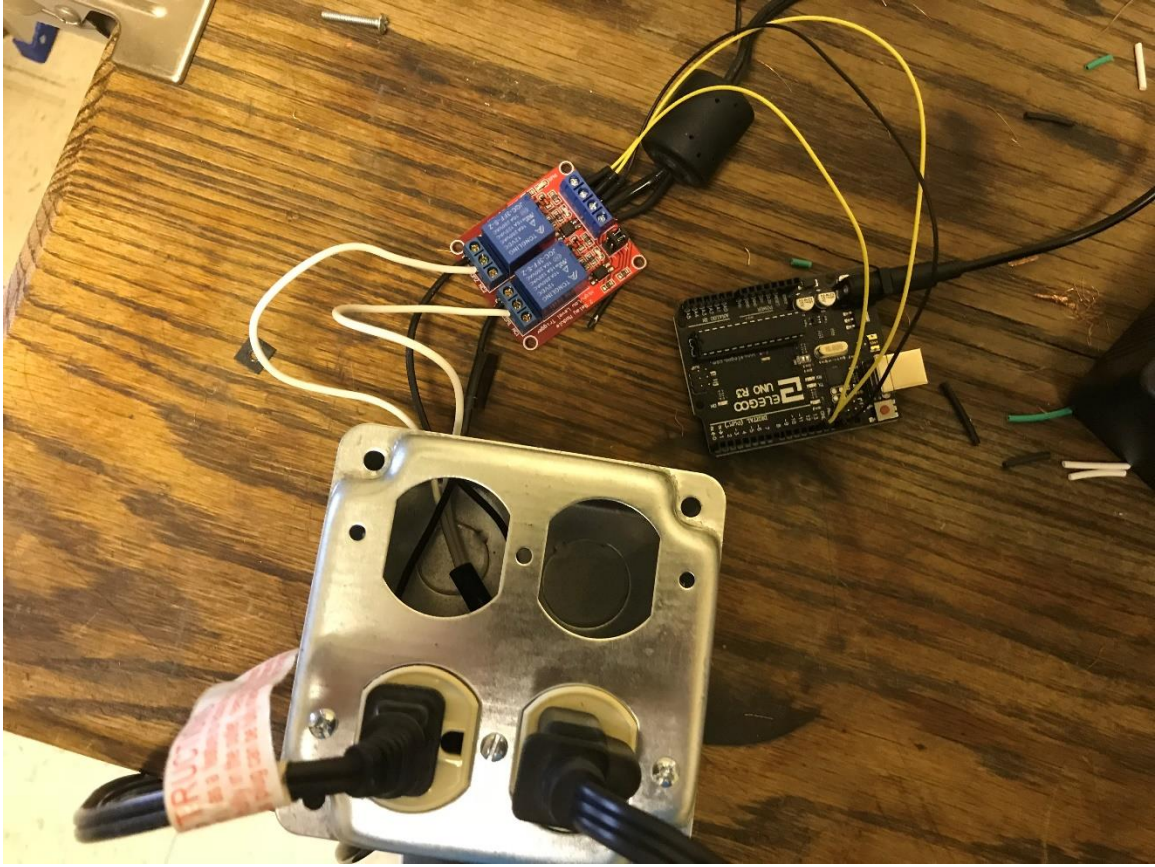
Figure 25: Repeat cycle timer made to automate the plating process.

3.7.3   Results and Discussion

All the images contain similar 20 μm scale bars. Given the 2-hour plating time, only a small number of the particles were expected to be plated and if they were plated, there was a potential that they would not be plated uniformly, as not all their sides may have had the opportunity to be exposed in the shortened experiment. Figure 26-28 display sections of the HF pretreated and coated powder. The results shown are consistent, in term of quality, with the powder that the sponsor supplied as the goal, shown in Figure 29.

المنارة للاستشارات

www.manaraa.com
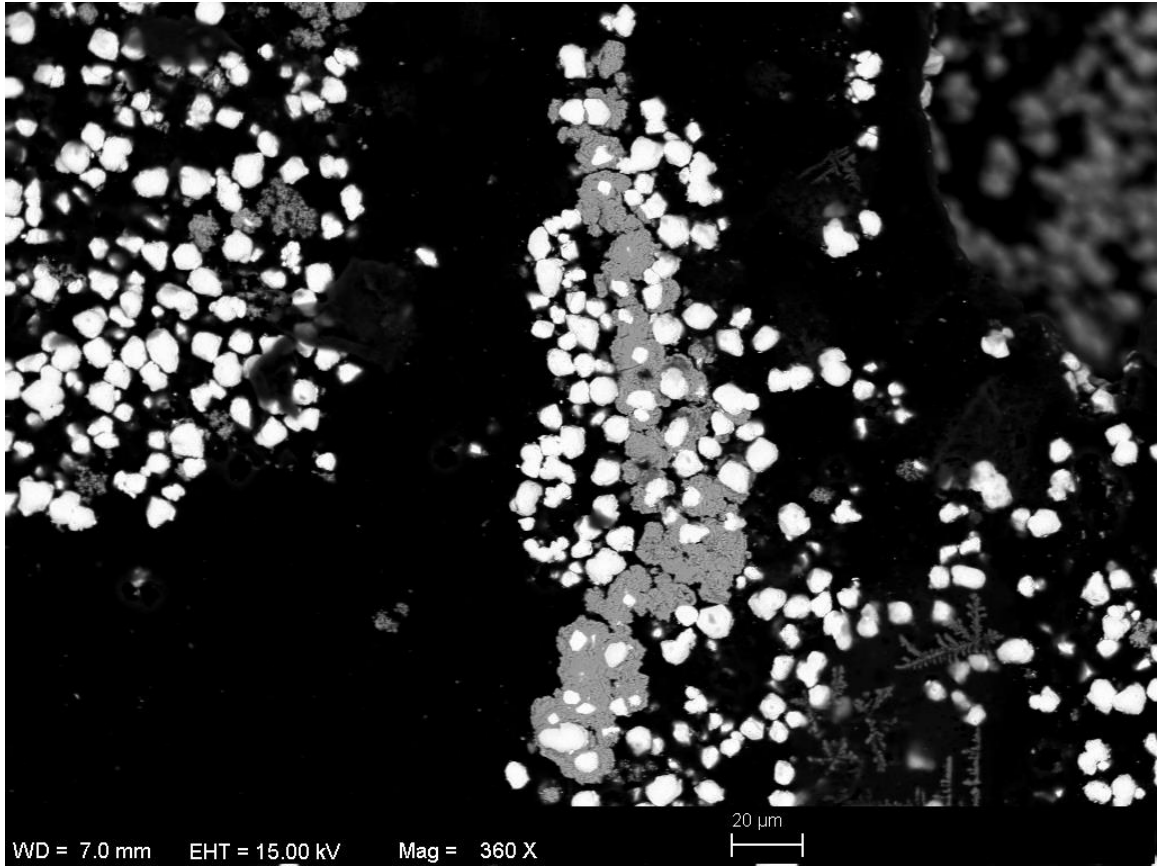
Figure 26: A section of the HF pretreated W powder electroplated at a current of 0.25A
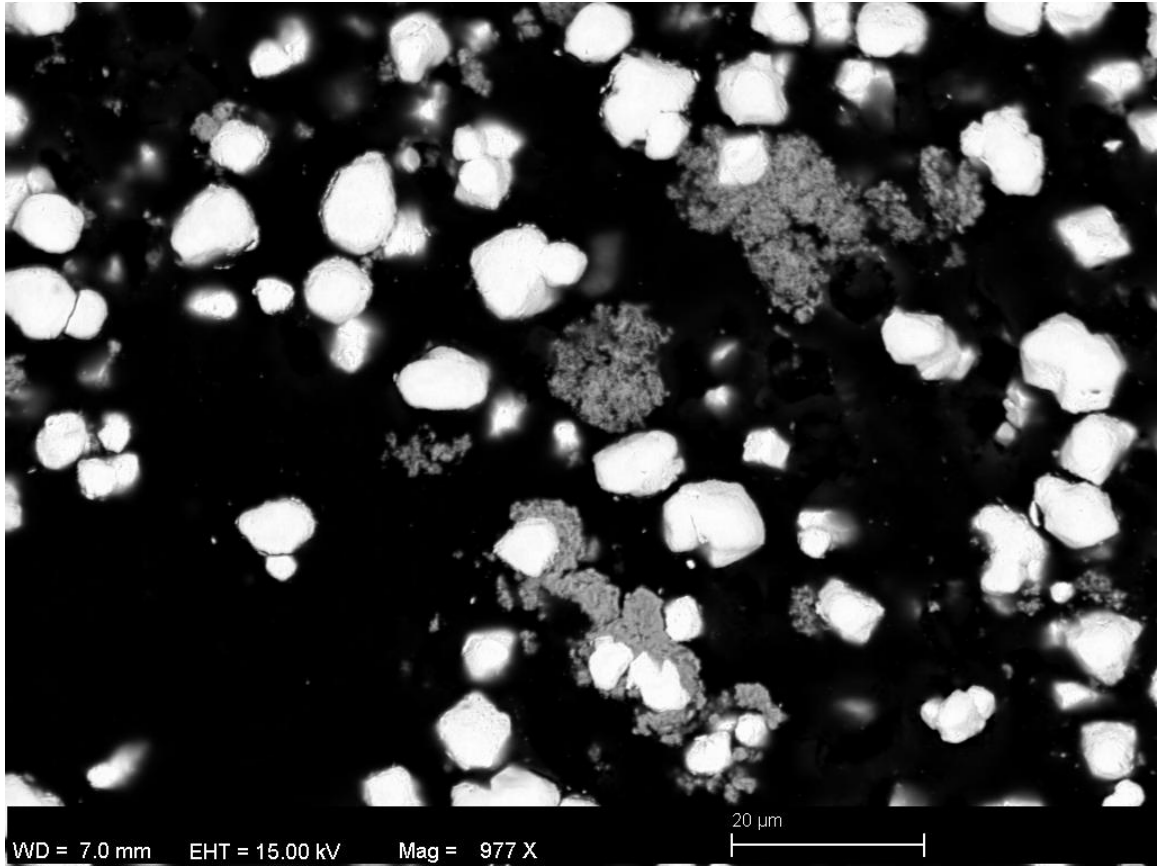
Figure 27: A section of the HF pretreated W powder electroplated at a current of 0.25A
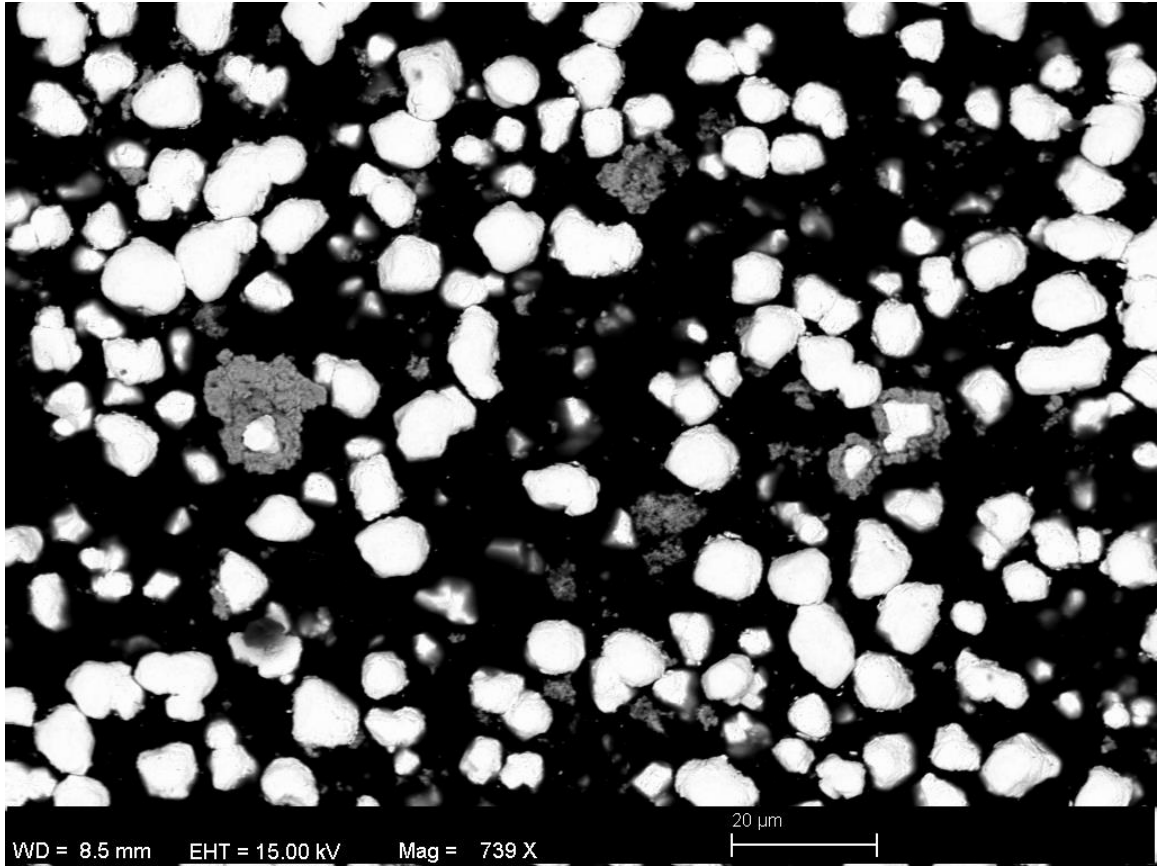
Figure 28: A section of the HF pretreated W powder electroplated at a current of 0.25A

Figures 26-28 show that the HF electro-etch pretreatment allows for the particles to be successfully deposited on. The particles in Figure 26 are slightly clumped into different copper casings, but they provide a similar appearance to those in Figure 29. As for Figures 27 and 28, many of the particles are not plated, but there are a few particles that were exposed or partially exposed in the 2-hour experiment that show good bonding between the W and Cu layers, indicating that the surface oxide layer was successfully removed, and plating could successfully take place over the entire surface and not just in the oxide layer gaps.

61
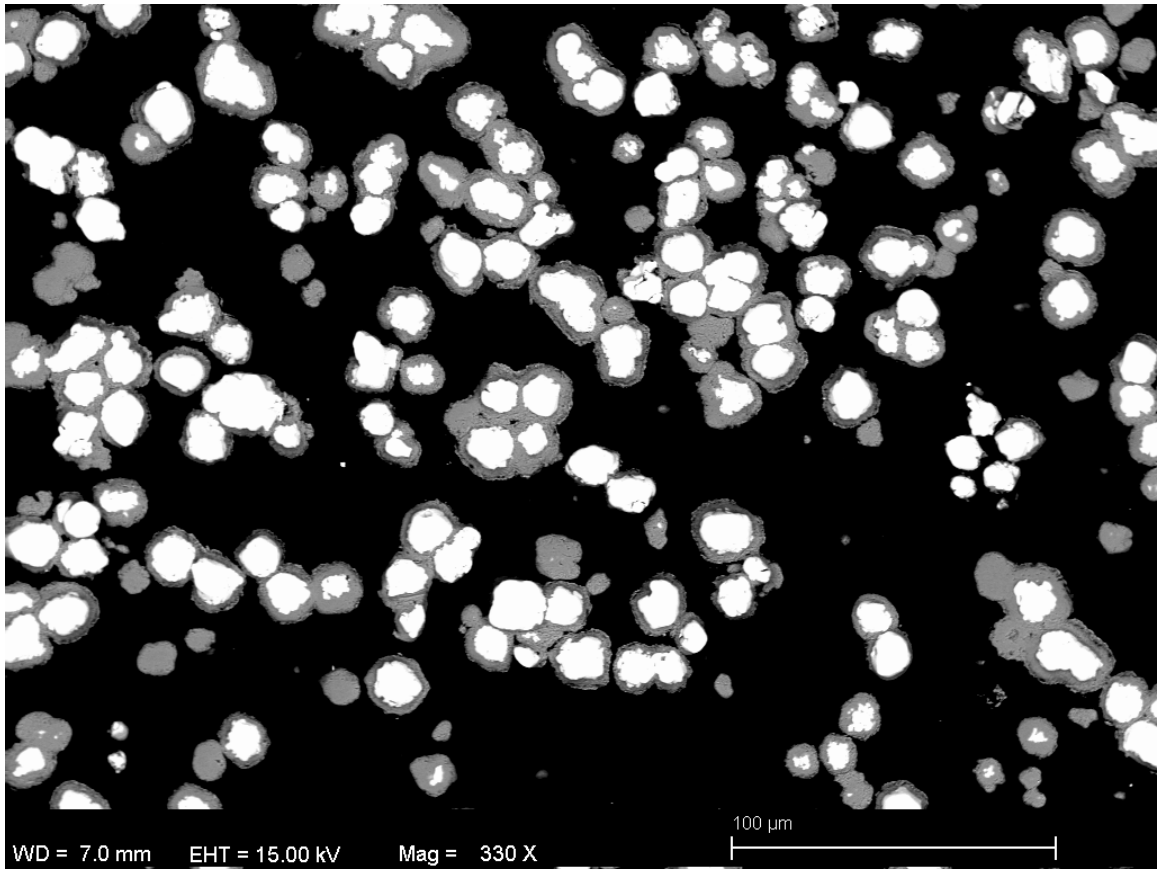
Figure 29: Provided sample of Cu coated W particle from the sponsor

The particles from Figures 26-28 do not appear to be as coated as those in Figure 29 and most of the particles in 29 appear to be coated, but it should be restated that in 26-28, the particles were only plated for 2 hours, where it would take over a day to plate them all. So, given more plating time, more of the particles from those figures would gain a copper coating. The HF test was only run at a low current, 0.25A, as this is the current that provided the best results previously and limited dendrite formation. Figure 30 displays another sample of coated particles from the HF experiment.
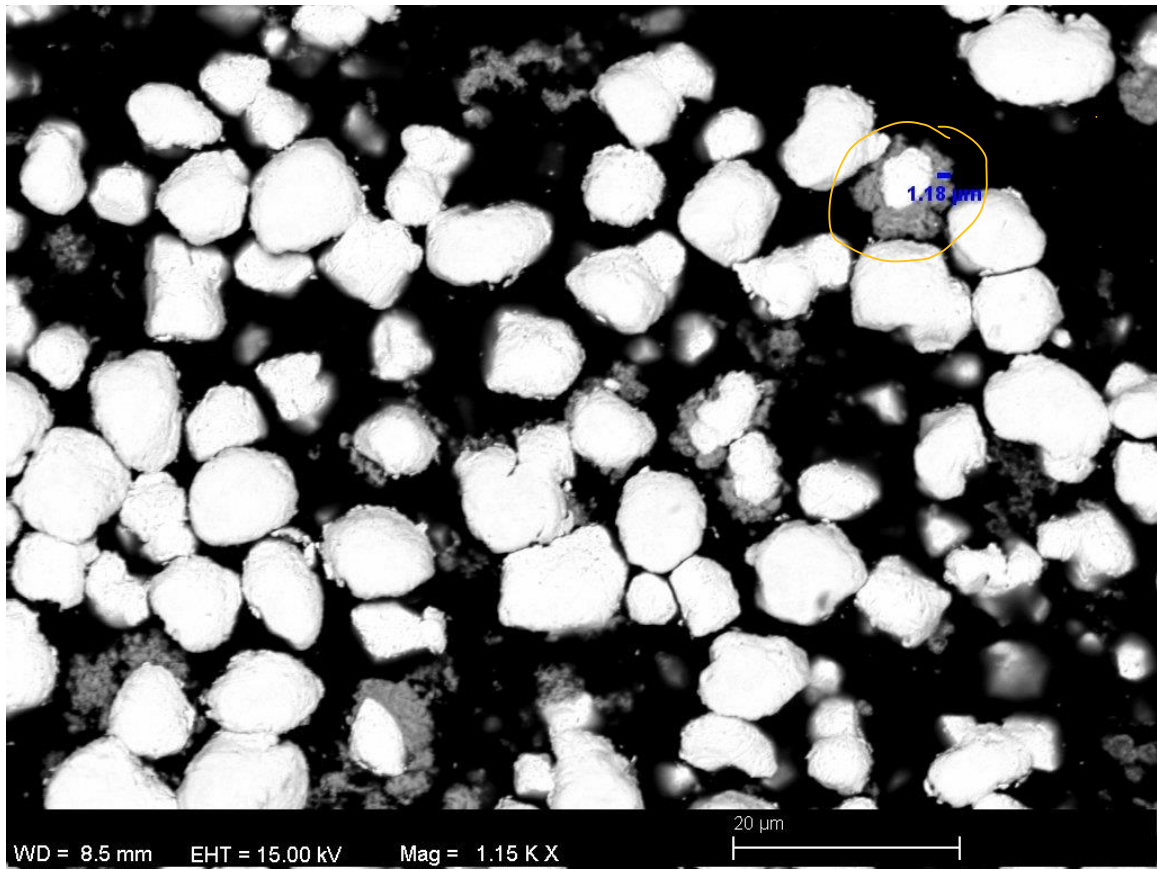
Figure 30: Another region of the HF pretreated particles showing some partial coating. The circled region is displaying the thickness of the coating.

The area presented in Figure 30 was not plated a sufficient amount during the 2-hour test. It provides a visual of partially plated, particles that maintain a solid bond with the copper. The copper in all these images was verified using EDS like that shown in Figure 6. The thickness of the plating is shown in the upper right of the figure to be 1.18 μm, close to the 1.48 μm thickness needed to obtain a 25% wt. Cu coating. While showing this, it also displays some mild agglomeration. The agglomeration in this experiment was significantly lower than that in all the other experiments and consistent with the sponsor's powder in Figure 29, where some agglomeration was seen. This figure further supported the idea that given more time, most of the particles would be

63

sufficiently plated in copper and the powder would more closely resemble that of Figure 29.

3.8   Conclusions

The W particles that were pretreated using an HF electro-etch yielded the finest results for electrodepositing copper onto W powder. Unfortunately, the goal of encasing all the W particles in 25% wt. Cu was not met yet. The HF pretreatment showed the ability to achieve coated particles in small quantities, but not at an industry level. A longer experiment time could yield many more coated particles and should be conducted to continually test the process.

The other powder pretreatment and the non-pretreated powder both unsuccessfully coated the W powder. The reason for the insufficient coating was due to a high local current density, with plating occurring in the gaps of the surface oxide layer. These results were supported by the foil tests conducted, proving that the HF pretreatment created the most favorable plating conditions and that the others created a coating that would peel away from the substrate.

Electrodeposition of copper onto the nickel coins showed a variation in the thickness of copper along the coin. This was attributed to slight current density differences along the coin, causing the areas of higher local current density to form larger copper deposits due to the area drawing a higher deposition rate.

The magnetic and paddle stirring methods provided an issue because each of the stirring methods caused a reduction of the cathode surface area. Therefore, the anode could not sufficiently plate on the entire powder surface. The methods of stirring for both

64

the magnetic and paddle stirrers need to be reassessed for future experimentation. If a new way of stirring is found that can eliminate the paddle through the copper end cap, then the cathode surface area can also be increased to increase plating efficiency.

Further work is necessary to reproduce the results seen in industry, or the sponsor's powder, as most of the particles in an industry sample are coated to the quality of the best of the particles obtained in this study.

CHAPTER 4

SUMMARY

Electroplating copper on W was a success on both the macroscopic and microscopic scales. On the macroscopic scale, the copper sulfate and H_2SO_4 electrolyte solution was successful for both the W foil and the nickel coins. The solution was tested on its ability to plate 23.4 μm onto the substrate, this amount of plating was accomplished over a 2-hour period at a constant current of 0.25A. The nickel was successfully plated with a 15.12 μm coating on the coin and a 20.97 μm coating on the W foil. The 23.4 μm coat was assuming a plating efficiency of 100%, but some copper was lost due to deposition onto the cathode and the formation of dendrites on the cathode that acted as high current density areas and attracted copper. The plating efficiencies seen in the foil test ranged from 83% to 91%.

The same copper sulfate solution was then used to coat W powder in microscopic electroplating experiments. All the experiments used a similar current between 0.25 and 3A, with the majority below 1A, as it was determined that deposition was more uniform at lower currents. Initial experiments used a magnetic stirring bar to mix the powder in solution with no additional agitation. These experiments contained non-pretreated powder and a nitric acid washed powder. These tests showed limited encapsulation of W particles in copper, due to an oxide layer on the surface of the particle that prevented the copper ions from bonding directly to the powder. Although, they did help in determining that the H_2SO_4 and copper sulfate electrolyte solution should be used over the HCl, and that the

lower current yielded a more uniform deposition. Once these two methods were ruled out, a second pretreatment method was added, an HF electro-etch.

Later experiments implemented the HF electro-etch with the addition of an ultrasonic bath and a new method of stirring the powder into the solution. The new experimental setup, along with the HF pretreatment, led to W particles being encased in copper at particle thicknesses between nearly 0 and 3 µm. The successful coatings from the HF experiment showed limited separation of W and Cu layers in the cross-sectional view, where the other experiments that appeared successful were slightly separated from their substrates, due to the oxide layer. Unlike the macroscopic substrate tests, the powder tests were cycled, to break up any copper bridges that may have formed during plating and to bring new particles to the top layer of powder. The cycle process is described in detail in Sections 2.3.1.3 and 3.2.2.

Although the powder coating tests were supposed to be run for over a day for all the particles to be theoretically coated, shortened tests were implemented for all pretreatments to determine the method was sufficient for plating the particles. Even though a shorter test was used, the repeat cycle timer created to automate the process was still used. The repeat cycle timer was also used for a full duration test of 24 hours to prove that it could sufficiently carry out the experiments.

In summation, only the HF electro-etch microscopic particle pretreatment successfully plated copper onto W powder with sufficient bonding between the W and Cu layers. The other two methods, nitric acid wash and no pretreatment, provided unsuccessful results that were able to direct the path to the HF etch. Each of these methods showed some coating, however, there was an oxide layer on the W powder still

that did not allow the copper ions to adhere to the powder surface. Also, both methods had a significant amount of copper agglomeration, as the copper could not plate onto the W particles. Although the HF pretreated particles still had some copper agglomeration in the results, it was significantly less than the other tests, and a comparable amount to that seen in the sponsor W-Cu powder BSE image in Figure 23. The HF pretreated particles can be seen in Figures 22 and 24. Some of the particles showed partial plating, due to the experiment duration only being 2 hours, when to plate the entire batch of powder it would take over 24. This led to only a small number of particles being plated and some being only partially plated, but the important note is the way the copper adheres to the particle surface with no layer in between, suggesting the oxide layer was removed by the electro-etch and successful plating had occurred. Had the duration of the experiment been longer, it was presumed that most of the remaining particles would be stirred to the top layer of powder and that their surfaces would be encapsulated as well.

CHAPTER 5

CONCLUSION

Preliminary experiments showed successful electrodeposition of Cu on W on a macroscopic and microscopic scale.

Some conditions reported in the literature as providing for success did not work for either W foil or powder, but one set worked. HF pretreatment showed the best results when combined with the copper sulfate and sulfuric acid bath solution for both macro and microscopic substrates. Nitric acid wash and non-pretreated powders were ruled out, as they did not produce successful coatings. This was attributed to an oxide layer remaining on the particles, where for the HF experiments, it was successfully removed.

Literature reports that an ultrasonic bath is necessary to keep particles agitated throughout the experiment to limit agglomeration. Tests confirmed that HF-pretreated powder plated in the presence of ultrasonic agitation had greatly reduced agglomeration, consistent with the literature. Tests were not performed to isolate the effects of these two changes.

The HF pretreated powder allowed good plating and showed promise for replicating the industrial powder that is no longer available. Additionally, the method of electrolytic deposition is a low-cost plating procedure that provides promise for use to obtain industry standard particles.

CHAPTER 6

FUTURE WORK

Encasing W particles in copper for cold spray is possible and should have further research put in to accomplishing this task. Electrolytic deposition of copper onto HF electro-etched W powder is currently the most promising method for coating powders for cold spray and further research should be conducted to make the process more efficient to achieve an even better result.

The first thing to be done moving forward is to test the experiment over its full duration and analyze the results to ensure most of the particles are getting uniformly plated with the desired thickness of copper. Once this has been determined, the apparatus should be improved to produce a more efficient plating result.

Currently, the stirring paddle is blocking a big portion of the cathode from a clear path for ions to move through the solution. Where the stirring mechanism is working, it is rigged together and a more permanent, sleek, design can take its place and increase the clear cathode surface area. The new method must still take place in an ultrasonic bath, as the constant agitation has been shown to increase plating efficiency. A modified set up with a lower profile stirrer or a magnetic stirring drive in an ultrasonic bath may prove more effective for electroplating.

Another improvement that should be made is the procedure for transferring the HF pretreated powder into the electrolyte bath. Polarization should be maintained for as long as possible and when taken away, be brought back as quickly as possible. The

70

current method of switching solutions in the beaker takes too long and causes some particles to react with the aqueous solutions to reform the oxide layer. So, a faster or more efficient method of transferring from the electro-etch to the electroplating would likely increase plating efficiency, as there would be less time for the W particles to reform an oxide layer.

Lastly, HF is a dangerous acid and needs to be handled with caution. It is worth searching for a way to remove the oxide without the use of HF to reduce the amount of safety equipment and training necessary to perform the test.

APPENDIX A

DRYING PROCEDURE FOR MICROSCOPIC PARTICLES

After the commencement of the electroplating:

- Sample filtered using vacuum filtration system (MILLIPORE Express Plus) that has an additional layer of filter paper (P5 was used for this experiment) to remove moisture until none was visible

- The filter paper from the funnel was removed and placed onto a petri dish

- Dish placed in vacuum desiccator, preventing the airflow from disrupting the particles after the moisture has been removed

- Allow the sample to sit in the desiccator for at least 1 hour

72

APPENDIX B

W POWDER PREPARATION PROCEDURE

After control testing, a nitric acid wash, was used in an attempt to remove surface contaminants and create a favorable, hydrophilic, surface for deposition. The procedure for the acid wash is:

- Create a 5:1 mixture of 70% nitric acid to powder in a glass beaker

- Allow the mixture to sit in the fume hood for 30 minutes

- Start a neutralization process by pouring mixture into a second glass beaker containing deionized water, give the powder time to settle at the bottom of the beaker

- Slowly pour the diluted mixture into a vacuum filtration system (MILLIPORE Express Plus) that has an additional layer of filter paper (P5 was used for this experiment) to assist in capturing all the powder

- Rinse the powder in the vacuum filter three additional times with deionized water

- Place the filter paper (P5) with the powder on it into a petri dish

- Place dish in vacuum desiccator for moisture removal

- Allow the dish to be in the desiccator for at least 1 hour

The second pretreatment, an electro-etch using HF, was used to remove the oxides from the particles surface before the electroplating process was executed. The etch procedure was approved for use by the ICSC committee and the approved document is as follows:

HF Lab Procedure for Etching Tungsten Foil and Powder
Presented for use by Richard Berdos under PI Robert Hyers in Gunness 10

The safety precautions laid out in the UMass Amherst Hydrofluoric Acid SOP as revised on
3-15-2018 will be followed throughout the duration of the experiment involving HF. The storage and waste procedures will also be carried out in accordance to this document. The procedure itself is intended to provide a surface etch on the Tungsten foil or powder to provide a more favorable plating surface for the copper.

<u>Equipment</u>
- Safety Equipment compliant with HF SOP
  - Neoprene Chemical Resistant Apron
  - Natural Rubber Gloves
  - Chemical Splash Goggles
  - Face Shield
- Lab Coat
- Nitrile Gloves (underneath HF compliant gloves)
- 250 mL HDPE Beaker
- 400 mL Glass Beaker
- HDPE Waste Jug
- HDPE Pipettes
- Hot Plate
- HDPE Secondary Containment
- AC Transformer
- Platinum Crucible
- W Foil/Powder
- Alligator Clips (soldered to rigid copper wire)
- Vacuum Filter
- Copper Foil (Powder only)
- Tape (to secure leads to fume hood frame)

Procedure

1. Ensure that the safety equipment used is compliant with the UMass Amherst HF SOP, including chemical splash goggles, a face shield, proper glove, and a chemical resistant splash apron. These should all be worn in addition to the standard lab coat and nitrile gloves.

2. Be sure that the fume hood is clear of all excess equipment and that only the essentials for the procedure remain inside the hood. Make sure to place a secondary containment PE bin into the fume hood where all HF use will take place, to ensure a facilitated clean up in the event of a spill.

3. This step is only for powder etching. Ensure that before the procedure is begun, the bottom of the HDPE beaker is fitted with a cathode for etching. This consists of a copper foil on the bottom of the beaker, with a small strip rising above the beaker so that a lead may be attached outside of the solution.

4. Inside of the PE container in the fume hood, place the 250 mL HDPE beaker inside of a 400 mL glass beaker for extra precaution. Fill the HDPE beaker with 90 mL of deionized water, which will be used to dilute the acid.

5. Using a PE pipette, dispense 10 mL of 50% HF into the 90 mL of deionized water in the HDPE beaker, creating a 100 mL solution of 5% HF. Dispose of the pipette as hazardous waste.

6. For foil, attach a long piece of foil to an alligator clip that is soldered to a rigid copper wire. The foil used should be approximately 3 times the length of the foil that will be plated, allowing for the alligator clip to remain out of the solution. For powder, using the cathode setup outlined in 3, carefully dispense the powder into the solution and allow it to settle to the bottom and contact the copper foil cathode.

7. Once the foil or powder insertion is complete, lower the platinum anode, attached to another alligator clip lead into the beaker. The anode should only be partially in the solution, ensuring that the clip itself is not in contact with the solution. This clip is also attached to a rigid copper lead, so both can be held in place away from the beaker itself. It is important to note that the anode and foil/powder should all be in contact with the solution, but not with each other.

8. Once the elements are secured, the power supply leads are ready to be attached. Wheel the power supply cart over to the fume hood. Once in position, lock the wheels to inhibit cart motion.

9. The power supply leads from the source should be taped to the frame of the fume hood. This will make certain that if the cart is moved, the strain will be relieved from the wires and the connection to the power source will be lost. This will prevent the contents in the hood from being disturbed and ensure that the HF is not spilled in the event of motion of the cart.

10. Once taped down, connect the leads to their respective anode and cathode leads on the rigid copper wires, the anode is the crucible and the cathode is the foil. Then, the HF etching process can begin.

11. The HF etching process will be carried out in accordance to patents US5456819A and US2443651A. The HF solution will be subjected to the voltages specified in the patents. During this process the HF solution is maintained at a temperature specified in the patent, using a hotplate, if needed, that is in the secondary containment.

12. Upon completion of the electro-etching, the foil shall be moved into the electroplating electrolyte bath and the electroplating process will commence. For powder samples, the contents will be filtered using a compatible vacuum filter, then dispensed into the electrolyte bath for electroplating.

13. The HF waste will then be placed into compatible HDPE jugs, labeled with proper hazardous waste tags and stored in a secondary containment bin in the lab. The HDPE beaker used has a spout to ensure a clean pour into the container.

14. Once completed, all safety equipment is removed, ensuring that none of it encounters the user. Be sure to dispose of any disposable items used in the correct way and follow the safety precautions outlined in the HF SOP.

APPENDIX C

CLEANING PROCEDURES

Standard cleaning procedure for glassware and equipment:

- Rinse beaker with small amount of DI water to remove left over drops from beaker or container

- Dispense a small amount of soap into the beaker or container, add a small amount of water and thoroughly clean the inside of the beaker with a steel wool sponge

- Fill beaker with hot water to ensure any leftover solution is neutralized

- Rinse objects with water at least three times or until the soap is gone

- In the event of residue still on the bottom of the beaker after this procedure, use a few drops of acetone mixed with water, be sure that this is done in the fume hood

- Allow the solution to sit for 5-10 minutes before diluting it by filling the beaker the rest of the way with DI water

- Dispose of acetone solution as waste, then repeat the initial cleaning with the steel wool sponge to remove the excess residue

77

REFERENCES

[1] P. Yih, "Method for Electroplating of micron Particulates with Metal Coatings". United States Patent 5911865, 11 April 1997.

[2] M. Schlesinger and M. Paunovic, "Electrodeposition of Copper," in *Modern Electroplating, fifth edition*, John Wiley & Sons, Inc., 2010, pp. 33-78.

[3] A guide to the use of lead for radiation shielding. (2017). *Lead Industries Association, Inc.*doi:10.18411/a-2017-023

[4] Hall, Aaron Christopher., et al. "Deposition Behavior in Cold Sprayed Copper-Tungsten Metal Matrix Composites." *Deposition Behavior in Cold Sprayed Copper-Tungsten Metal Matrix Composites. (Conference) | OSTI.GOV*, 1 Jan. 2015, www.osti.gov/servlets/purl/1244889.

[5] Army Reasearch Lab Center for Cold Spray, "ARL Center for Cold Spray - Advantages," United States Army Research Laboratory, 19 May 2015. [Online]. Available: http://www.arl.army.mil/www/default.cfm?page=371. [Accessed 11 March 2018].

[6] "Properties of Tungsten." *Buffalo Tungsten Inc. Tungsten Powder Homepage*, www.buffalotungsten.com/index.html.

[7] *Safety Data Sheet Tungsten Powder;* Buffalo Tungsten Inc., Depew, NY, Aug 16, 2016. (accessed Mar 11, 2018).

[8] Xu, Jiudong, et al. "Preparation of Copper Coated Tungsten Powders by Intermittent Electrodeposition." *Powder Technology*, vol. 264, 2014, pp. 561–569., doi:10.1016/j.powtec.2014.06.005.

[9] G. DiBari, "Electrodeposition of Nickel," in *Modern Electroplating*, Wiley & Sons, Inc., 2010, pp. 79-110.

[10] B. Nejad, "Role of PH & temperature in bright nickel(Watts) plating," Linkden, 14 July 2014. [Online]. Available: https://www.linkedin.com/pulse/20140724171711-252588790-role-of-ph-temperature-in-bright-nickel-watts-plating. [Accessed 11 March 2018].

[11] Rigali, J.R. (2017). ELECTROLESS DEPOSITION & ELECTROPLATING OF NICKEL ON CHROMIUM-NICKEL CARBIDE POWDER (Master's thesis).

[12] K. C. Wilson, G. R. Addie, A. Sellgren and R. Clift, "Chapter 2 Review of fluid and particle mechanics," in *Slurry Transport Using Centrifugal Pumps*, Springer US, 2006, pp. 15-50.

[13] Lashmore, D. and Kelley, D. (1995). *PROCESS FOR ELECTRODEPOSITING METAL AND METAL ALLOYS ON TUNGSTEN, MOLYBDENUMAND OTHER DFFICULT TO PLATE METALS*. US5456819.